

# Future neutrino oscillation facilities

A. Blondel<sup>a</sup>, A. Cervera-Villanueva<sup>a</sup>, A. Donini<sup>b</sup>, P. Huber<sup>c</sup>, M. Mezzetto<sup>d</sup>, P. Strolin<sup>e</sup>

<sup>a</sup> *Section de Physique, Université de Genève, Switzerland*

<sup>b</sup> *I.F.T. and Dep. Física Teórica, U.A.M., Madrid, Spain*

<sup>c</sup> *Department of Physics, University of Wisconsin*

<sup>d</sup> *INFN, Sezione di Padova, Italy*

<sup>e</sup> *Università degli Studi e Sezione INFN, Napoli, Italy*

## Abstract

The recent discovery that neutrinos have masses opens a wide new field of experimentation. Accelerator-made neutrinos are essential in this program. Ideas for future facilities include high intensity muon neutrino beams from pion decay ('SuperBeam'), electron neutrino beams from nuclei decays ('Beta Beam'), or muon and electron neutrino beams from muon decay ('Neutrino Factory'), each associated with one or several options for detector systems. Each option offers synergetic possibilities, e.g. some of the detectors can be used for proton decay searches, while the Neutrino Factory is a first step towards muon colliders. A summary of the perceived virtues and shortcomings of the various options, and a number of open questions are presented.

## 1 Physics of massive neutrinos

### 1.1 Status

Neutrino physics has become one of the most active areas of research in particle physics. There are many reasons for this development, one of the most important is that neutrino physics is a data driven field – for several years now, new data are pouring at an astounding rate. It began in 1987 with the first detection of supernova neutrinos. Although only 19 events were observed [1, 2], they allowed to confirm the standard picture of core-collapse supernovæ. Furthermore those 19 events also constitute the detection of the oldest neutrinos ever; they were produced some 150 000 years ago. The fact that there were detectable neutrinos after this time allows to put stringent bounds on the neutrino life time. Furthermore the environment at the production site was a very special one – a dense and hot proto-neutron star. This offers the possibility to derive strong bounds on any additional interaction neutrinos could have. A comprehensive review on the properties of neutrinos which can be deduced from supernovæ is given in [3].

In 1998 Super-K's atmospheric neutrino data [4] gave the first clear evidence for neutrino oscillation. This result was a real turning point for neutrino physics. Neutrino oscillation implies that neutrinos do have a mass and the finding that the mixing angle is large was completely unexpected. In analogy to the quark sector the common belief was that if neutrinos mixed at all then the mixing angles should be small. The importance of the Super-K result is that it is the first strong evidence for physics beyond the Standard Model. With the Super-K result the number of publications per year containing the word neutrino in their title four-folded<sup>1</sup>.

The year 2002 was an annus mirabilis for neutrino physics. The solar neutrino puzzle was proven to be due to the properties of the neutrino and not of the Sun. The neutral current data of SNO [5] yielded an independent determination of the total flux of active neutrinos from the Sun and in combination with other solar neutrino data proved that solar neutrinos undergo a flavor transition. Kamland [6]

<sup>1</sup>According to the hep-ph preprint server of arXive.org

provided an independent check of the oscillation hypothesis by using reactor neutrinos and constrained the mixing parameters to the so called LMA solution. These two results together are extremely difficult to explain other than by neutrino oscillation. Also the evidence for oscillation in atmospheric neutrinos has been confirmed independently by K2K [7,8], which is the first long baseline experiment. Furthermore two pioneers of neutrino physics were awarded the Nobel prize. Masatoshi Koshiba was awarded one fourth of the prize for the detection of neutrinos from a supernova and Ray Davis Jr. was awarded another fourth for his detection of solar neutrinos. A relatively recent review on the topic of neutrino oscillations in general is given in *e.g.* [9].

The above experiments indicate the presence of two mass splittings  $\Delta m_{21}^2$  and  $\Delta m_{31}^2$ , corresponding to solar and atmospheric neutrino oscillations, in agreement with existence of three active neutrinos. There has been a further experiment observing evidence for neutrino oscillation – LSND. The results of this experiment indicate that there is a third mass splitting  $\Delta m_{\text{LSND}}^2$  in the range  $0.2 - 10 \text{ eV}^2$  [10]. The Karmen experiment [11] on the other hand excludes a large part of the parameter region claimed by LSND. In a combined analysis of both data sets there still remains a combined allowed region [12]. The third mass splitting cannot be accommodated within a three neutrino flavor framework. Basically two possible solutions exist – either there are more than three neutrinos, which means that the additional neutrinos are sterile in order not to create a conflict with the decay width of the  $Z^0$  (see *e.g.* [13]), or there is a huge CPT-violation, which would make the mass splittings of neutrinos and of anti-neutrinos independent of each other. Both solutions suffer from phenomenological problems, *i.e.* they do not fit the existing data very well. Finally Miniboone will thoroughly test the results of LSND. A fairly recent review of neutrino physics is to be found in [14], which also contains an extensive bibliography.

The current parameters are roughly

$$\begin{aligned} \Delta m_{21}^2 &\sim 8 \cdot 10^{-5} \text{ eV}^2 & \text{and} & \theta_{12} \sim 1/2 \\ \Delta m_{31}^2 &\sim 2 \cdot 10^{-3} \text{ eV}^2 & \text{and} & \theta_{23} \sim \pi/4 \\ & & & \theta_{13} \lesssim 0.15 \end{aligned} \tag{1}$$

This implies a lower bound on the mass of the heaviest neutrino  $\sqrt{2 \cdot 10^{-3} \text{ eV}^2} \sim 0.04 \text{ eV}$  but we currently do not know which neutrino is the heaviest. For a more detailed global analysis of the data see *e.g.* [15]. We now can contrast our knowledge of the neutrino mixing with the quark sector

$$U_{CKM} = \begin{pmatrix} 1 & 0.2 & 0.005 \\ 0.2 & 1 & 0.04 \\ 0.005 & 0.04 & 1 \end{pmatrix} \quad U_\nu = \begin{pmatrix} 0.8 & 0.5 & ? \\ 0.4 & 0.6 & 0.7 \\ 0.4 & 0.6 & 0.7 \end{pmatrix} \tag{2}$$

The mixing of neutrinos is very different from that of quarks, since there are two large mixing angles. Neutrino masses are also peculiar because they are at least five orders of magnitude smaller than the mass of the electron. These facts pose a major challenge to any theory of neutrino masses and mixings: Why are neutrino masses so small? Why is the neutrino mixing pattern so different from that of the quarks? What is the pattern of neutrino masses?

## 1.2 Origin of neutrino mass

The Standard Model is in a paradox situation – it is extremely successful in describing elementary particles and their interactions and still it is strongly believed to be incomplete. It seems to be the correct description of the physics which can be observed at low energies but it is obvious from its structure that it cannot be correct up to the very highest energies. This has inspired many attempts to provide a

convincing model for the physics beyond the Standard Model. These attempts strongly suffered from the fact that no deviation from the Standard Model had been found before the discovery of neutrino flavor transitions. The discovery of neutrino oscillations is the first unequivocal experimental result which is beyond the SM. Neutrinos within the SM are strictly massless, *i.e.* it is impossible to write down a mass term for the neutrino which is gauge invariant and renormalizable.

One possibility to approach this problem can be formulated in the language of effective field theory. The SM is believed to be an effective field theory, which means it is only valid up to some energy scale  $\Lambda$ . At this scale new physics and degrees of freedom will appear. In the absence of a full theory for the new physics one still can write down a parameterization of the effects of the new physics in terms of non-renormalizable (within the SM) operators

$$\mathcal{L}_{SM} + \frac{1}{\Lambda} \mathcal{L}_5 + \frac{1}{\Lambda^2} \mathcal{L}_6 + \dots \quad (3)$$

where the higher dimensional operators are suppressed by increasing powers of  $\Lambda$ . In general there can be a large number of operators of a given dimension, *e.g.* there are many dimension 6 operators, among them is the one responsible for proton decay. In that picture the first correction to the SM is expected to come from the dimension 5 operators  $\mathcal{L}_5$  since they are only suppressed by one power of  $\Lambda$ . It turns out that there is only one dimension 5 operator, given by

$$\mathcal{L}_5 = \frac{1}{\Lambda} (LH)(LH) \rightarrow \frac{1}{\Lambda} (L\langle H \rangle)(L\langle H \rangle). \quad (4)$$

This operator is the neutrino mass operator. The fact that neutrino mass is the first correction to the SM which is expected from theory and found in experiment is a interesting coincidence.

Technically it is straightforward to generate the neutrino mass operator by introducing new degrees of freedom. The most commonly used choice are heavy right handed neutrinos  $N_R$ , which are singlets under the SM gauge group. In that case it becomes possible to write down a Majorana mass for the neutrinos

$$\mathcal{L}_\nu = m_D \bar{\nu}_L N_R + \frac{1}{2} m_R \bar{N}_L^c N_R + h.c.. \quad (5)$$

This construction yields light neutrino masses of the order

$$m_\nu \simeq \frac{m_D^2}{m_R}, \quad (6)$$

which is the famous seesaw relation. Putting a typical fermion mass of  $m_D = 100 \text{ GeV}$  and  $m_R = 10^{15} \text{ GeV}$  at the GUT scale yields a neutrino mass of order  $0.01 \text{ eV}$ . This value is tantalizing close to the order of magnitude indicated by oscillations. In this scheme the smallness of neutrino masses is natural consequence of the heaviness of the right handed neutrino. In such a scenario neutrino masses are a probe of very high energy scales which may otherwise be not accessible. It turns out that it is far from trivial to construct a theory which can account for the observed mixing pattern, *i.e.* predict two large mixing angles. The seesaw mechanism is just one example and there a plethora of other possibilities. For some reviews on the vast amount of literature on these topics see [16–21].

### 1.3 Baryogenesis

The observable Universe only contains matter and no anti-matter. This is a very surprising experimental fact since the initial condition are thought to be symmetric with respect to matter and anti-matter.

**Table 1:** Predictions for certain oscillation related quantities from various textures of the neutrino mass matrix under the assumption of a diagonal lepton mass matrix. Adapted from [21].

Case	Texture	Hierarchy	$ U_{e3} $	$ \cos 2\theta_{23} $	Solar Angle
A	$\frac{\sqrt{\Delta m_{13}^2}}{2} \begin{pmatrix} 0 & 0 & 0 \\ 0 & 1 & 1 \\ 0 & 1 & 1 \end{pmatrix}$	Normal	$\sqrt{\frac{\Delta m_{12}^2}{\Delta m_{13}^2}}$	$\sqrt{\frac{\Delta m_{12}^2}{\Delta m_{13}^2}}$	$\mathcal{O}(1)$
B	$\sqrt{\Delta m_{13}^2} \begin{pmatrix} 1 & 0 & 0 \\ 0 & \frac{1}{2} & -\frac{1}{2} \\ 0 & -\frac{1}{2} & \frac{1}{2} \end{pmatrix}$	Inverted	$\frac{\Delta m_{12}^2}{ \Delta m_{13}^2 }$	$\frac{\Delta m_{12}^2}{ \Delta m_{13}^2 }$	$\mathcal{O}(1)$
C	$\frac{\sqrt{\Delta m_{13}^2}}{\sqrt{2}} \begin{pmatrix} 0 & 1 & 1 \\ 1 & 0 & 0 \\ 1 & 0 & 0 \end{pmatrix}$	Inverted	$\frac{\Delta m_{12}^2}{ \Delta m_{13}^2 }$	$\frac{\Delta m_{12}^2}{ \Delta m_{13}^2 }$	$ \cos 2\theta_{12}  \sim \frac{\Delta m_{12}^2}{ \Delta m_{13}^2 }$
Anarchy	$\sqrt{\Delta m_{13}^2} \begin{pmatrix} 1 & 1 & 1 \\ 1 & 1 & 1 \\ 1 & 1 & 1 \end{pmatrix}$	Normal	$> 0.1$	–	$\mathcal{O}(1)$

Baryogenesis aims at finding an explanation for the observed matter anti-matter asymmetry. It turns out that within the SM model it is in principle very well possible to create some asymmetry but the numerical value is way too small. For that reason this asymmetry points to physics beyond the SM. More surprisingly, the same new physics which is invoked to explain neutrino masses may be at the heart of baryogenesis. Assuming that the Universe was hot enough at some point in its history to keep  $N_R$  in thermal equilibrium there will be a vast abundance of  $N_R$ . The  $N_R$  will fall out of equilibrium during the evolution and finally decay. This decay can be CP-violating and therefore produce a net lepton number

$$\Gamma(N_R \rightarrow LH) - \Gamma(N_R \rightarrow \bar{L}H^*) \neq 0. \quad (7)$$

This lepton number later on will be converted to baryon number by non-perturbative processes.

#### 1.4 Phenomenological consequences

In the context of GUT scale right handed neutrinos it is very difficult to establish a one-to-one correspondence between high and low-energy observables. A given model, however, usually has generic predictions for low energy observables. Therefore studying neutrinos allows to gain considerable insight into phenomena which otherwise would be inaccessible. Colliders can not probe this kind of physics, since any effects in scattering amplitudes are suppressed by  $m_{GUT}$ , at LHC this would be effects of  $\mathcal{O}(10^{-10})$ ! In general any model of neutrino mass should provide predictions for the mixing pattern and the mass scale as well as whether neutrinos are Majorana or Dirac particles. In terms of flavor physics and the quest for a theory of flavor neutrinos provide one half of the available data.

Based on consideration like the one summarized in table 1 it is possible to identify a set of key measurements necessary to identify credible scenarios for neutrino mass generation. Another example are  $SO(10)$  GUT models, which typically make quite precise predictions for  $|U_{e3}|$ . The most sensitive low energy observables and the environment to measure them are

- Majorana vs Dirac mass –  $0\nu\beta\beta$
- Absolute  $m_\nu$  – Katrin, Cosmology

- How large is  $\theta_{13}$ ? – Oscillation
- Which one is the heaviest neutrino?  $-0\nu\beta\beta$ , Katrin, Oscillation
- Is  $\theta_{23}$  maximal? – Oscillation
- Is there leptonic CP violation? – Oscillation
- Are there only 3 light neutrinos? – Oscillation

If MiniBooNE should find evidence for a forth neutrino the last item would move up to number one and it would change our view on neutrinos and model building profoundly. What is remarkable about that list is that a large number of items can be studied by neutrino oscillation.

Massive neutrinos offer a variety of fascinating new phenomenology beyond oscillation. A rather extensive review on the wide area of neutrinos in cosmology is given in [22]. Cosmology has undergone a tremendous increase in the available experimental data as well and is now entering a phase of high precision measurements. With the data of WMAP [23] and the 2dFGRS [24] the cosmological limits on the masses of neutrinos are already slightly better than the laboratory bounds, see *e.g.* [25].

In order to develop and finally test a theory of neutrino masses and mixing it will be essential to further improve on the knowledge of not only the oscillation parameters but also the absolute mass scale of neutrinos. Furthermore the observation of neutrino-less double  $\beta$ -decay could shed some light onto the Majorana nature of neutrinos. The theoretical motivation, the current status and future experiments for neutrino-less double  $\beta$ -decay are reviewed in [26, 27], whereas the prospects of determining the absolute mass scale are reviewed in [28].

## 1.5 Neutrino oscillation

The mass eigenstates are related to flavor eigenstates by  $U_\nu$ , thus a neutrino which is produced as flavor eigenstate is a superposition of mass eigenstates. These mass eigenstates propagate with different velocity and a phase difference is generated. This phase difference gives rise to a finite transition probability

$$P_{\nu_\alpha \rightarrow \nu_\beta} = \sum_{ij} U_{\alpha j} U_{\beta j}^* U_{\alpha i}^* U_{\beta i} e^{-i \frac{\Delta m_{ij}^2 L}{2E}} \quad (8)$$

Neutrino oscillation is a quantum mechanical interference phenomenon and therefore it is uniquely sensitive to extremely tiny effects.

In order to get some qualitative understanding it is useful to use the two flavor approximation, *i.e.* only one mass splitting  $\Delta m^2$  and one mixing angle  $\theta$ . In that case the oscillation probabilities take the simple form

$$\begin{aligned} P_{\nu_\alpha \rightarrow \nu_\beta} &= \sin^2 2\theta \sin^2 \left( \frac{\Delta m^2 L}{4E} \right), \\ P_{\nu_\alpha \rightarrow \nu_\alpha} &= 1 - \sin^2 2\theta \sin^2 \left( \frac{\Delta m^2 L}{4E} \right), \end{aligned} \quad (9)$$

where  $L$  is the distance traveled by the neutrinos and is usually called baseline and  $E$  is the neutrino energy.  $P_{\nu_\alpha \rightarrow \nu_\beta}$  is called appearance probability, since the flavor  $\beta$  appears as final state and analogously  $P_{\nu_\alpha \rightarrow \nu_\alpha}$  is called disappearance probability, since the flavor  $\alpha$  disappears. Obviously the two probabilities fulfill the unitarity condition  $P_{\nu_\alpha \rightarrow \nu_\beta} + P_{\nu_\alpha \rightarrow \nu_\alpha} = 1$ . Moreover  $P_{\nu_\alpha \rightarrow \nu_\beta}$  is invariant

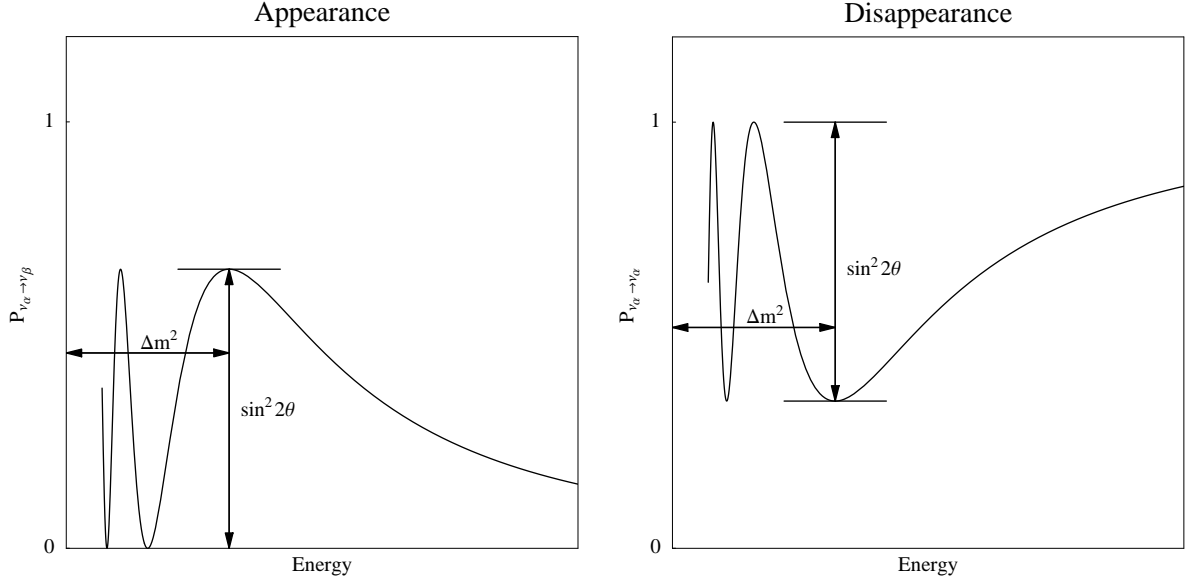


**Figure 1:** The oscillation probability as a function of the energy in arbitrary units. The left hand panel shows the signature of the mixing angle  $\theta$  (vertical arrow) and the one of the mass splitting  $\Delta m^2$  (horizontal arrow) in the case of an appearance experiment, whereas the right hand panel shows the signatures in the case of a disappearance experiment.

under time reversal and CP-conjugation, since in the two neutrino case there is no CP violation in neutrino oscillations for the same reason as there would be no CP violation in the quark sector if only two families existed [29].

The parameters  $\Delta m^2$  and  $\theta$  are fundamental constants like the electron mass or the Cabibbo-angle. However the baseline and neutrino energy can in principle be chosen by the experimental setup. The signature for the value of the mixing angle in an appearance experiment, *i.e.* an experiment which observes  $P_{\nu_\alpha \rightarrow \nu_\beta}$ , is given by the height of the oscillation peak, which is also indicated by the vertical arrow in the left hand panel of Figure 1. The value of  $\Delta m^2$  is given by the position of the oscillation peak as a function of the energy, which is shown as horizontal arrow. For a disappearance experiment the oscillation peak becomes an oscillation dip as shown in the right hand panel of Figure 1. The depth of the dip is now the signature for the mixing angle as indicated by the vertical arrow. The position of the dip yields the value of the mass splitting and is indicated by the horizontal arrow.

For both kinds of experiments, appearance and disappearance, there can be a correlation between the measured values of  $\Delta m^2$  and  $\theta$ , *i.e.* an error on the determination of one parameter introduces an additional uncertainty on the other parameter. Furthermore an experiment needs to have enough energy resolution to clearly determine the position of the peak, otherwise the experiment sees an energy independent signal proportional to  $1/2 \sin^2 2\theta$ . Another important factor for the determination of the mass splitting is the energy calibration of the detector – any error on the absolute energy scale directly translates into an error in the position of the oscillation peak or dip. The major difference between the two possible experiments is that an appearance experiment is much more sensitive to small values of  $\theta$ , because the measurement is performed relative to zero, whereas a disappearance experiment measures relative to unity. This implies a different behavior of the two types of experiments with respect to certain systematical errors. On the one hand, the level of background is crucial for an appearance

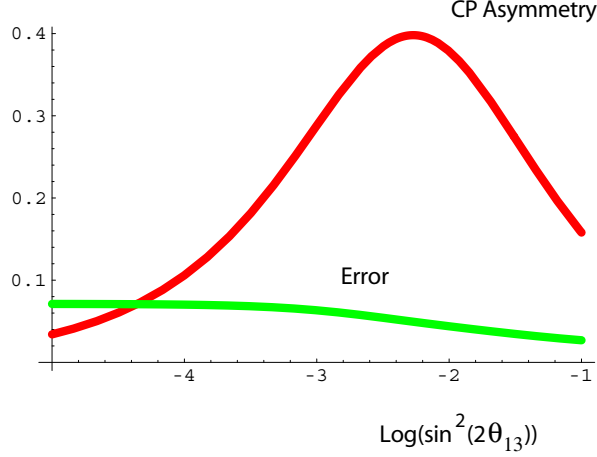


**Figure 2:** Magnitude of the CP asymmetry at the first oscillation maximum, for  $\delta = 1$  as a function of the mixing angle  $\sin^2 2\theta_{13}$ . The curve marked 'error' indicates the dependence of the statistical+systematic error on such a measurement. The curves have been computed for the baseline Beta Beam option at the fixed energy  $E_\nu = 0.4$  GeV,  $L=130$  km, statistical + 2% systematic errors.

experiment, since a large background reduces the sensitivity to small values of  $\theta$ . On the other hand, the total normalization is vital for a disappearance measurement, because a large normalization error makes it impossible to detect deviations from unity.

In the full three flavor case, like in the quark sector mixing can cause CP violation

$$P(\nu_\alpha \rightarrow \nu_\beta) - P(\bar{\nu}_\alpha \rightarrow \bar{\nu}_\beta) \neq 0 \quad (10)$$

The size of this effect is proportional to

$$J_{CP} = \frac{1}{8} \cos \theta_{13} \sin 2\theta_{13} \sin 2\theta_{23} \sin 2\theta_{12} \sin \delta \quad (11)$$

The experimentally most suitable transition to study CP violation is  $\nu_e \leftrightarrow \nu_\mu$ , basically because there are techniques to produce beams of  $\nu_\mu$  or  $\bar{\nu}_\mu$  as well as detectors for them. In any case energies above the muon threshold are needed, which are only available in beam experiments. A common tool to gain some insight into how CP effects are measured is the use of the so called CP asymmetry  $A_{CP}$ :

$$A_{CP} = \frac{P(\nu_\mu \rightarrow \nu_e) - P(\bar{\nu}_\mu \rightarrow \bar{\nu}_e)}{P(\nu_\mu \rightarrow \nu_e) + P(\bar{\nu}_\mu \rightarrow \bar{\nu}_e)} \quad (12)$$

displayed in Fig. 2, or the equivalent time reversal asymmetry  $A_T$ .

The asymmetry can be large and its value increases for decreasing values of  $\theta_{13}$  up to the value when the two oscillations (solar and atmospheric) are of the same magnitude. The following remarks can be made:

1. The ratio of the asymmetry to the statistical error is fairly independent on  $\theta_{13}$  for large values of this parameter, which explains the relative flatness of the sensitivity curves.
2. This asymmetry is valid for the first maximum. At the second oscillation maximum the curve is shifted to higher values of  $\theta_{13}$  so that it could be then an interesting possibility for measuring the CP asymmetry, although the reduction in flux is considerable (roughly factor 9).

3. The asymmetry has opposite sign for  $\nu_e \rightarrow \nu_\mu$  and  $\nu_e \rightarrow \nu_\tau$ , and changes sign when going from one oscillation maximum to the next.
4. The asymmetry is small for large values of  $\theta_{13}$  placing a challenging emphasis on systematics.

In many cases the propagation of neutrinos does not take place in vacuo but in matter. Although the interaction of neutrinos with matter is tiny, matter can have a substantial impact on the oscillation probabilities. The weak interaction couples the neutrinos to matter and besides hard scattering events there is also coherent forward scattering in very much the same fashion as for visible light traveling through glass. The point is that the coherent forward scattering amplitudes are not the same for all neutrino flavors, since ordinary matter is made of particles of the first family and does specifically not contain muons or tau-leptons. All flavors have the same amplitude for neutral current reactions but the electron neutrinos have an additional contribution due to charged current reactions. The electron (anti-)neutrino is the only one which can scatter coherently with the electrons in the matter via the charged current and this yields an additional contribution to the potential  $A$  for electron (anti-)neutrinos of

$$A = (-)2\sqrt{2}G_F n_e E, \quad (13)$$

where  $G_F$  is the Fermi coupling constant,  $n_e$  is the electron density and  $E$  is the neutrino energy. The minus sign is for anti-neutrinos. In matter the Schrödinger equation for neutrino propagation is now modified by a term containing the potential  $A$ . This potential gives rise to an additional phase for  $\nu_e$  and thus changes the oscillation probability. This has two consequences:

$$A_{CP} \neq 0 \quad (14)$$

even if  $\delta = 0$ , since the potential distinguishes neutrinos from anti-neutrinos. The second consequence of the matter potential is that there can be a resonant conversion – the MSW effect. The condition for the resonance is

$$\Delta m^2 \simeq A \quad (15)$$

Obviously the occurrence of this resonance depends on the signs of both sides in this equation. Thus oscillation becomes sensitive to the mass ordering

	$\nu$	$\bar{\nu}$
$\Delta m^2 > 0$	MSW	-
$\Delta m^2 < 0$	-	MSW

The general, exact expression for the three flavor oscillation probabilities in matter [30] is rather long and does therefore not provide much insight. Without going into the details it is noteworthy that the  $\nu_e$  to  $\nu_\mu$  transition has the richest structure in terms of effects which in principle can be extracted. This, however, also implies that there are strong correlations, especially between  $\delta_{CP}$  and  $\theta_{13}$  [31]. Moreover, there can be up to eight discrete, degenerate solutions [32]. This problem has been widely recognized and a large number of solutions have been proposed like including additional final states, *e.g.*  $\nu_\tau$  or to use different energies and baselines.

## 1.6 Neutrino mass limits from laboratories

Direct laboratory limits on neutrino masses are obtained from kinematical studies. The most stringent current upper limit is that on the  $\bar{\nu}_e$  mass, coming from the Mainz experiment measuring the end-point of the electron energy spectrum in Tritium beta decay [33]

$$m_{\bar{\nu}_e} \leq 2.2 \text{ eV (95\%CL)}$$



The Troitsk group has also published a similar limit [34]:

$$m_{\bar{\nu}_e} \leq 2.1 \text{ eV (95\%CL)}$$

however they must include an ad-hoc step function near the endpoint to avoid the problem of negative mass squared.

The proposed KATRIN experiment aims to improve the sensitivity to  $m_{\bar{\nu}_e} \sim 0.3 \text{ eV}$  [35]. Similar sensitivities are the goal of the longer term MARE experiment [36] based on an array of several thousand of microbolometers. These measurements are sensitive to:

$$m_{\bar{\nu}_e} = \left( \sum_i |U_{ei}^2| m_i^2 \right)^{1/2} = \left( \cos^2 \theta_{13} (m_1^2 \cos^2 \theta_{12} + m_2^2 \sin^2 \theta_{12}) + m_3^2 \sin^2 \theta_{13} \right)^{1/2} \quad (16)$$

Limits to neutrino masses come also from cosmology [44], combining results from cosmic microwave anisotropies, supernovae surveys, galaxy clustering and Lyman  $\alpha$  cloud absorption power, limits on the sum of the neutrino masses of the order of 1 eV can be derived.

An important constraint on Majorana neutrino masses arises from neutrinoless double- $\beta$  decay, in which an  $(A, Z)$  nucleus decays to  $(A, Z + 2) + 2 e^-$ , without any neutrino emission. This process can be used to constrain the combination

$$|m_{\beta\beta}| = \left| \sum_i U_{ei}^{*2} m_i \right| = \left| \cos^2 \theta_{13} (m_1 \cos^2 \theta_{12} + m_2 e^{2i\alpha} \sin^2 \theta_{12}) + m_3 e^{2i\beta} \sin^2 \theta_{13} \right|. \quad (17)$$

which involves a coherent sum over all the different Majorana neutrino masses  $m_i$ , weighted by their mixings with the electron flavour eigenstate, which may include CP-violating phases, as discussed below. This observable is therefore distinct from the quantity observed in Tritium  $\beta$  decay.

The interpretation of neutrinoless double- $\beta$  decay data depends on calculations of the nuclear matrix elements entering in this process.

A claim for a neutrinoless double- $\beta$  signal has been made by [37] analyzing the Heidelberg-Moscow data on  $^{76}\text{Ge}$ :

$$T_{1/2}^{0\nu} = 1.19 \cdot 10^{25} \text{ years}$$

corresponding to

$$< m_{\beta\beta} > = 0.05 - 0.85 \text{ eV (95\%CL)}$$

the uncertainty coming from the choice of the nuclear matrix element calculation.

This result is in contrast with the limit computed with a combined analysis of a subset of the Heidelberg-Moscow data and IGEX experiments [38] and to what reported by a separate group of the original collaboration [39], reporting no evidence for a signal.

Recent results on  $^{130}\text{Te}$  from the Cuoricino collaboration [40]:  $T_{1/2}^{0\nu} > 1.8 \cdot 10^{24} \text{ years}$  corresponding to  $m_{\beta\beta} < .2 - 1.1 \text{ eV}$  and on  $^{100}\text{Mo}$  from the NEMO3 collaboration [41]:  $T_{1/2}^{0\nu} > 4.6 \cdot 10^{23} \text{ years}$  corresponding to  $m_{\beta\beta} < .7 - 2.8 \text{ eV}$  do not confirm the Germanium claim, but are not sensitive enough to rule out it.

The approved future experiments at LNGS CUORE [42] and GERDA [43] will have the required sensitivity to unambiguously clarify this experimental situation: having a sensitivity of  $m_{\beta\beta} = 0.024 - 0.14 \text{ eV}$  and  $m_{\beta\beta} = 0.09 - 0.29 \text{ eV}$  respectively.

## 2 Description of the accelerator neutrino facilities

### 2.1 Present generation of long-baseline experiments

<sup>2</sup> Over the next five years the present generation of oscillation experiments at accelerators with long-baseline  $\nu_\mu$  beams (Table 2), K2K at KEK [57], MINOS [66] at the NuMI beam from FNAL [67] and ICARUS [68] and OPERA [69] at the CNGS beam from CERN [70] are expected to confirm the atmospheric evidence of oscillations and measure  $\sin^2 2\theta_{23}$  and  $|\Delta m_{23}^2|$  within  $10 \div 15$  % of accuracy if  $|\Delta m_{23}^2| > 10^{-3} \text{ eV}^2$ . K2K and MINOS are looking for neutrino disappearance, by measuring the  $\nu_\mu$  survival probability as a function of neutrino energy while ICARUS and OPERA will search for evidence of  $\nu_\tau$  interactions in a  $\nu_\mu$  beam, the final proof of  $\nu_\mu \rightarrow \nu_\tau$  oscillations. K2K has already completed its data taking at the end of 2004, while MINOS has started data taking beginning 2005. CNGS is expected to start operations in the second half of 2006.

**Table 2:** *Main parameters for present long-baseline neutrino beams*

Neutrino facility	Proton momentum (GeV/c)	L (km)	$E_\nu$ (GeV)	pot/yr ( $10^{19}$ )
KEK PS	12	250	1.5	2
FNAL NuMI	120	735	3	$20 \div 34$
CERN CNGS	400	732	17.4	$4.5 \div 7.6$

In all these facilities conventional muon neutrino beams are produced through the decay of  $\pi$  and  $K$  mesons generated by a high energy proton beam hitting needle-shaped light targets. Positive (negative) mesons are sign-selected and focused (defocused) by large acceptance magnetic lenses into a long evacuated decay tunnel where  $\nu_\mu$ 's ( $\bar{\nu}_\mu$ 's) are generated. In case of positive charge selection, the  $\nu_\mu$  beam has typically a contamination of  $\bar{\nu}_\mu$  at few percent level (from the decay of the residual  $\pi^-$ ,  $K^-$  and  $K^0$ ) and  $\sim 1\%$  of  $\nu_e$  and  $\bar{\nu}_e$  coming from three-body  $K^\pm$ ,  $K_0$  decays and  $\mu$  decays. The precision on the evaluation of the intrinsic  $\nu_e$  to  $\nu_\mu$  contamination is limited by the knowledge of the  $\pi$  and  $K$  production in the primary proton beam target. Hadroproduction measurements at 400 and 450 GeV/c performed with the NA20 [71] and SPY [72] experiments at the CERN SPS provided results with  $5 \div 7\%$  intrinsic systematic uncertainties.

The CNGS  $\nu_\mu$  beam has been optimized for the  $\nu_\mu \rightarrow \nu_\tau$  appearance search. The beam-line design was accomplished on the basis of the previous experience with the WANF beam at CERN SPS [73]. The expected muon neutrino flux at the Gran Sasso site will have an average energy of 17.4 GeV and  $\sim 0.6\%$   $\nu_e$  contamination for  $E_\nu < 40$  GeV. Due to the long-baseline ( $L=732$  Km) the contribution to neutrino beam from the  $K^0$  and mesons produced in the reinteraction processes will be strongly reduced with respect to the WANF [74]: the  $\nu_e/\nu_\mu$  ratio is expected to be known within  $\sim 3\%$  systematic uncertainty [75].

Current long-baseline experiments with conventional neutrino beams can look for  $\nu_\mu \rightarrow \nu_e$  even if they are not optimized for  $\theta_{13}$  studies. MINOS at NuMI is expected to reach a sensitivity of  $\sin^2 2\theta_{13} = 0.08$  [66] integrating  $14 \cdot 10^{20}$  protons on target (pot) in 5 years according to the FNAL proton plan evolution [76]. MINOS main limitation is the poor electron identification efficiency of the detector.

Thanks to the dense ECC structure and the high granularity provided by the nuclear emulsions, the OPERA detector is also suited for electron and detection [69]. The resolution in measuring the energy of an electromagnetic shower in the energy range relevant to CNGS is approximately constant

<sup>2</sup>Material for this Section is mainly taken from ref. [65]

and is about 20%. Furthermore, the nuclear emulsions are able to measure the number of grains associated to each track. This allows an excellent two tracks separation (better than  $1 \mu\text{m}$ ). Therefore, it is possible to disentangle single-electron tracks from tracks produced by electron pairs coming from  $\gamma$  conversion in the lead. These features are particularly important for the  $\nu_\mu \rightarrow \nu_e$  analysis. The outstanding position resolution of nuclear emulsions can also be used to measure the angle of each charged track with an accuracy of about 1 mrad. This allows momentum measurement by using the Multiple Coulomb Scattering with a resolution of about 20% and the reconstruction of kinematical variables characterizing the event (i.e. the missing transverse momentum at the interaction vertex  $p_T^{\text{miss}}$  and the transverse momentum of a track with respect to hadronic shower direction  $Q_T$ ).

The expected number of events for the  $\nu_\mu \rightarrow \nu_e$  oscillation search is reported in Table 3

**Table 3:** Expected number of signal and background events and analysis efficiencies  $\epsilon$  for OPERA [77, 78] assuming 5 years data taking with the nominal CNGS beam and oscillation parameters  $\Delta m_{23}^2 = 2.5 \times 10^{-3} \text{ eV}^2$ ,  $\theta_{23} = 45^\circ$  and  $\theta_{13} = 5^\circ$ .

$\theta_{13}$	$\sin^2 2\theta_{13}$	$\nu_e \text{CC signal}$	$\tau \rightarrow e$	$\nu_\mu \text{CC} \rightarrow \nu_\mu \text{NC}$	$\nu_\mu \text{NC}$	$\nu_e \text{CC beam}$
$7^\circ$	0.058	5.8	4.6	1.0	5.2	18
$\epsilon$		0.31	0.032	$3.4 \cdot 10^{-5}$	$7 \cdot 10^{-5}$	0.082

OPERA can reach a 90% C.L. sensitivity  $\sin^2 2\theta_{13} = 0.06$  ( $\Delta m_{23}^2 = 2.5 \cdot 10^{-3} \text{ eV}^2$ , convoluted to CP and matter effects) [77, 78], a factor  $\sim 2$  better than Chooz for five years exposure to the CNGS beam at nominal intensity for shared operation  $4.5 \cdot 10^{19}$  pot/yr.

A plot of  $\theta_{13}$  sensitivities is reported in Fig. 3. According to the CERN PS and SPS upgrade studies [79], the CNGS beam intensity could be improved by a factor 1.5, allowing for more sensitive neutrino oscillation searches for the OPERA experiment.

It is worth mentioning that the sensitivity on  $\theta_{13}$  measurement of the current long-baseline experiments with conventional neutrino beams, like NuMI and CNGS, will be limited by the power of the proton source which determines the neutrino flux and the event statistics, by the not optimized  $L/E_\nu$  and by the presence of the  $\nu_e$  intrinsic beam contamination and its related systematics. This is particular true for CNGS where the neutrino energy, optimized to overcome the kinematic threshold for  $\tau$  production and to detect the  $\tau$  decay products, is about ten times higher the optimal value for  $\theta_{13}$  searches at that baseline.

Another approach to search for non vanishing  $\theta_{13}$  is to look at  $\bar{\nu}_e$  disappearance using nuclear reactors as neutrino source.

The Double-Chooz experiment aims at improving the current knowledge on  $\theta_{13}$  by observing the disappearance of  $\bar{\nu}_e$  from nuclear reactors. The relevant oscillation probability is

$$P(\bar{\nu}_e \rightarrow \bar{\nu}_e) \simeq 1 - \sin^2 2\theta_{13} \sin^2 \left( \frac{\Delta m_{31}^2 L}{4E} \right) + \dots \quad (18)$$

which does not depend on  $\theta_{23}$  and the CP-phase  $\delta_{CP}$ . The dependence on  $\Delta m_{21}^2$  and  $\theta_{12}$  is negligible for the chosen baseline. Therefore this approach allows a unambiguous detection of  $\theta_{13}$  free of correlations and degeneracies. As it is obvious from eq. 18 the measurement requires a very precise control of the absolute flux. For that reason Double-Chooz will employ a near and far detector. The direct comparison of the event rates in each detector will allow to cancel many systematical errors and thus is essential in reaching the required low level of residual errors. Both detectors need some overburden

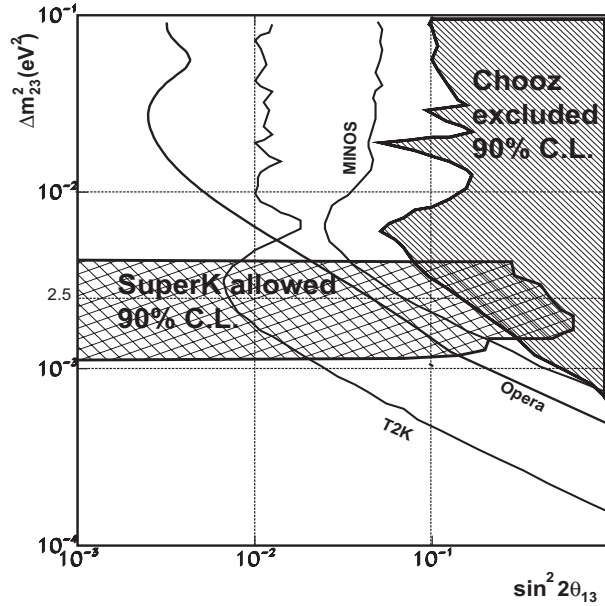


**Figure 3:** Expected sensitivity on  $\theta_{13}$  mixing angle (matter effects and CP violation effects not included) for MINOS, OPERA and for the next T2K experiment, compared to the Chooz exclusion plot, from [65].

to reduce the cosmic muon flux to an acceptable level. The advantage of Double-Chooz is that it will use an existing cavern for the far detector, which puts it ahead in time of any other reactor experiment, provided that the final funding decision is made in a timely manner. This cavern is 1.05 km away from

**Table 4:** Overview of the systematic errors of the CHOOZ and Double-CHOOZ experiment. Table taken from [80]

	CHOOZ	Double-CHOOZ
Reactor cross section	1.9 %	—
Number of protons	0.8 %	0.2 %
Detector efficiency	1.5 %	0.5 %
Reactor power	0.7 %	—
Energy per fission	0.6 %	—

the reactor and the near detector will be at  $\sim 200$  m from the reactor. Both detectors will be based on a Gadolinium loaded liquid scintillator and use inverse  $\beta$ -decay and the delayed neutron capture signal. Both detector will have a fiducial mass of 10.16 t. The improvements in systematical accuracy need are summarized in table 4.

The sensitivity after 5 years of data taking will be  $\sin^2 2\theta_{13} = 0.02$  at 90% CL [80], which could be achieved as early as 2012. It is conceivable to use a larger, second cavern to place a 200 t detector to even improve that bound down to  $\sin^2 2\theta_{13} < 0.01$  [81].

A sketch of  $\theta_{13}$  sensitivities as a function of the time, following the schedule reported in the experimental proposals, computed for the approved experiments, is reported in Fig. 4.

According to the present experimental situation, conventional neutrino beams can be improved and optimized for the  $\nu_\mu \rightarrow \nu_e$  searches. The design of a such new SuperBeam facility for a very high

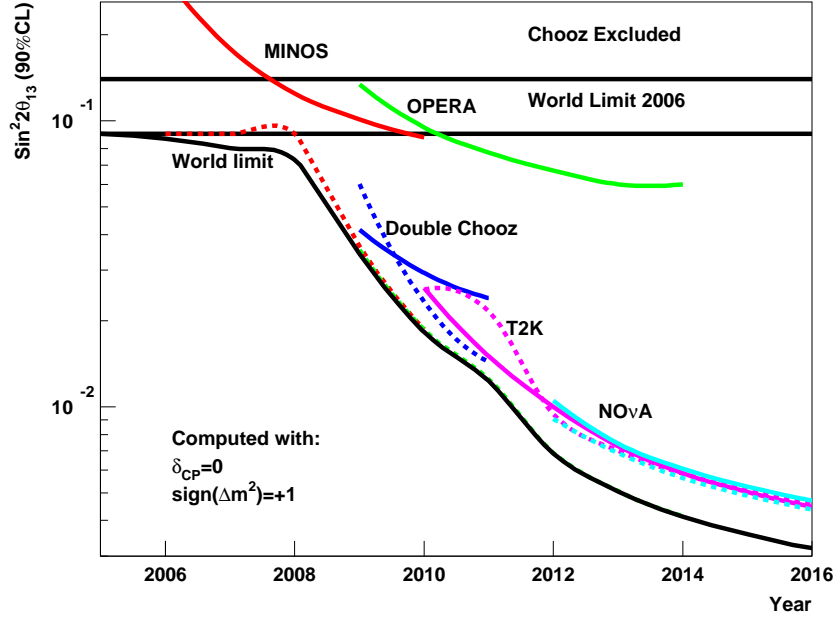


**Figure 4:** Evolution of sensitivities on  $\sin^2 2\theta_{13}$  as function of time. For each experiment are displayed the sensitivity as function of time (solid line) and the world sensitivity computed without the experiment (dashed line). The comparison of the two curves shows the discovery potential of the experiment along its data taking. The world overall sensitivity along the time is also displayed. The comparison of the overall world sensitivity with the world sensitivity computed without a single experiment shows the impact of the results of the single experiment. Experiments are assumed to provide results after the first year of data taking.

intensity and low energy  $\nu_\mu$  flux will demand:

- a new higher power proton driver, exceeding the megawatt, to deliver more intense proton beams on target;
- a tunable  $L/E_\nu$  in order to explore the  $\Delta m_{23}^2$  parameter region as indicated by the previous experiments with neutrino beams and atmospheric neutrinos;
- narrow band beams with  $E_\nu \sim 1 \div 2$  GeV;
- a lower intrinsic  $\nu_e$  beam contamination which can be obtained suppressing the  $K^+$  and  $K^0$  production by the primary proton beam in the target.

An interesting option for the SuperBeams is the possibility to tilt the beam axis a few degrees with respect to the position of the far detector (Off-Axis beams) [94,95]. According to the two body  $\pi$ -decay kinematics, all the pions above a given momentum produce neutrinos of similar energy at a given angle  $\theta \neq 0$  with respect to the direction of parent pion (contrary to the  $\theta = 0$  case where the neutrino energy is proportional to the pion momentum). These neutrino beams have several advantages with respect to the corresponding on-axis ones: they are narrower, lower energy and with a smaller  $\nu_e$  contamination (since  $\nu_e$  mainly come from three body decays) although the neutrino flux can be significantly smaller.

The intrinsic limitations of conventional neutrino beams are overcome if the neutrino parents can be fully selected, collimated and accelerated to a given energy. This can be attempted within the

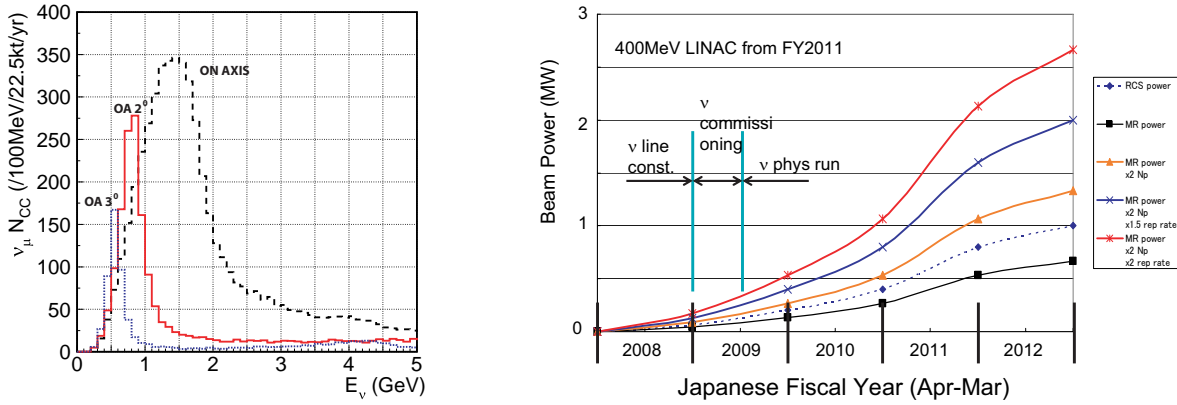


**Figure 5:** Left: T2K neutrino beam energy spectrum for different off-axis angle  $\theta$ . Right: expected evolution of T2K beam power as function of time. Baseline option is the second lowest solid curve.

muon or a beta decaying ion lifetimes. The neutrino beams from their decays would then be pure and perfectly predictable. The first approach brings to the Neutrino Factories [96], the second to the BetaBeams [97]. However, the technical difficulties associated with developing and building these novel conception neutrino beams suggest for the middle term option to improve the conventional beams by new high intensity proton machines, optimizing the beams for the  $\nu_\mu \rightarrow \nu_e$  oscillation searches (SuperBeams).

## 2.2 Off axis SuperBeams: T2K, T2HK and NO $\nu$ A

The T2K (Tokai to Kamioka) experiment [94] will aim neutrinos from the Tokai site to the Super-Kamiokande detector 295 km away. The neutrino beam is produced by pion decay from a horn focused beam, with a system of three horns and reflectors. The decay tunnel length (130 m long) is optimized for the decay of 2-8 GeV pions and short enough to minimize the occurrence of muon decays. The neutrino beam is situated at an angle of 2-3 degrees from the direction of the Super-Kamiokande detector, assuring a pion decay peak energy of 0.6 GeV. The beam line is equipped with a set of dedicated on-axis and off-axis near detectors at the distance of 280 meters.

The main goals of the experiment are as follows:

1. The highest priority is the search for  $\nu_e$  appearance to detect sub-leading  $\nu_\mu \rightarrow \nu_e$  oscillations. It is expected that the sensitivity of the experiment in a 5 years  $\nu_\mu$  run, will be of the order of  $\sin^2 2\theta_{13} \leq 0.006$  [94].
2. Disappearance measurements of  $\nu_\mu$ . This will improve measurement of  $\Delta m_{23}^2$  down to a precision of a  $0.0001 \text{ eV}^2$  or so. The exact measurement of the maximum disappearance is a precise measurement of  $\sin^2 2\theta_{23}$ . These precision measurements of already known quantities require good knowledge of flux shape, absolute energy scale, experimental energy resolution and of the cross-section as a function of energy. They will be crucial to measure the tiny  $\nu_\mu \rightarrow \nu_e$  oscillations [98,99].
3. Neutral current disappearance (in events tagged by  $\pi^0$  production) will allow for a sensitive search of sterile neutrino production.

The T2K experiment is planned to start in 2009 with a beam intensity reaching 1 MW beam power on target after a couple years, see Fig. 5. It has an upgrade path which involves: a further near detector

station at 2 km featuring a water Čerenkov detector, a muon monitor and a fine grain detector (possibly liquid argon). The phase II of the experiment, often called T2HK, foresees an increase of beam power up to the maximum feasible with the accelerator and target (4 MW beam power), antineutrino runs, and a very large water Čerenkov (HyperKamiokande) with a rich physics programme in proton decay, atmospheric and supernova neutrinos and, perhaps, leptonic CP violation, that could be built around in about 15-20 years from now.

The NO $\nu$ A experiment with an upgraded NuMI Off-Axis neutrino beam [100] ( $E_\nu \sim 2$  GeV and a  $\nu_e$  contamination lower than 0.5%) and with a baseline of 810 Km (12 km Off-Axis), has been recently proposed at FNAL with the aim to explore the  $\nu_\mu \rightarrow \nu_e$  oscillations with a sensitivity 10 times better than MINOS. If approved in 2006 the experiment could start data taking in 2011. The NuMI target will receive a 120 GeV/c proton flux with an expected intensity of  $6.5 \cdot 10^{20}$  pot/year ( $2 \cdot 10^7$  s/year are considered available to NuMI operations while the other beams are normalized to  $10^7$  s/year). The experiment will use a near and a far detector, both using liquid scintillator (TASD detector). In a 5 years  $\nu_\mu$  run, with 30 kton active mass far detector, a sensitivity on  $\sin^2 2\theta_{13}$  slightly better than T2K, as well as a precise measurement of  $|\Delta m_{23}^2|$  and  $\sin^2 2\theta_{23}$ , can be achieved. NO $\nu$ A can also allow to solve the mass hierarchy problem for a limited range of the  $\delta_{CP}$  and  $\text{sign}(\Delta m_{23}^2)$  parameters [100]. As a second phase, the new proton driver of 8 GeV/c and 2 MW, could increase the NuMI beam intensity to  $17.2 \div 25.2 \cdot 10^{20}$  pot/year, allowing to improve the experimental sensitivity by a factor two and to initiate the experimental search for the CP violation.

### 2.3 SPL SuperBeam

In the CERN-SPL SuperBeam project [116–118] the planned 4MW SPL (Superconducting Proton Linac) would deliver a 2.2 GeV/c proton beam, on a Hg target to generate an intense  $\pi^+$  ( $\pi^-$ ) beam focused by a suitable magnetic horn in a short decay tunnel. As a result an intense  $\nu_\mu$  beam, will be produced mainly via the  $\pi$ -decay,  $\pi^+ \rightarrow \nu_\mu \mu^+$  providing a flux  $\phi \sim 3.6 \cdot 10^{11} \nu_\mu/\text{year}/\text{m}^2$  at 130 Km of distance, and an average energy of 0.27 GeV. The  $\nu_e$  contamination from  $K$  will be suppressed by threshold effects and the resulting  $\nu_e/\nu_\mu$  ratio ( $\sim 0.4\%$ ) will be known within 2% error. The use of a near and far detector (the latter at  $L = 130$  Km of distance in the Frejus area [119], see Sec. 3.3.1) will allow for both  $\nu_\mu$ -disappearance and  $\nu_\mu \rightarrow \nu_e$  appearance studies. The physics potential of the 2.2 GeV SPL SuperBeam (SPL-SB) with a water Čerenkov far detector with a fiducial mass of 440 kton, has been extensively studied [117].

New developments show that the potential of the SPL-SB potential could be improved by rising the SPL energy to 3.5 GeV [120], to produce more copious secondary mesons and to focus them more efficiently. This seems feasible if status of the art RF cavities would be used in place of the previously foreseen LEP cavities [121].

The focusing system (magnetic horns), originally optimized in the context of a Neutrino Factory [122, 123], has been redesigned considering the specific requirements of a Super Beam. To obtain a maximum oscillation probability, corresponding to a mean neutrino energy of 300 MeV, one should collect 800 MeV/c pions, see Fig. 6. At higher beam energy, the kaon rates grow rapidly compared to the pion rates, an experimental confirmation [92] of such numbers would be strongly needed.

In this upgraded configuration neutrino flux could be increased by a factor  $\sim 3$  with respect to the 2.2 GeV configuration, the number of expected  $\nu_\mu$  charged current is about 95 per kton  $\cdot$  yr

A sensitivity  $\sin^2 2\theta_{13} < 0.8 \cdot 10^{-3}$  is obtained in a 5 years  $\nu_\mu$  plus 5 year  $\bar{\nu}_\mu$  run ( $\delta = 0$  intrinsic degeneracy accounted for, sign and octant degeneracies not accounted for), allowing to discovery CP

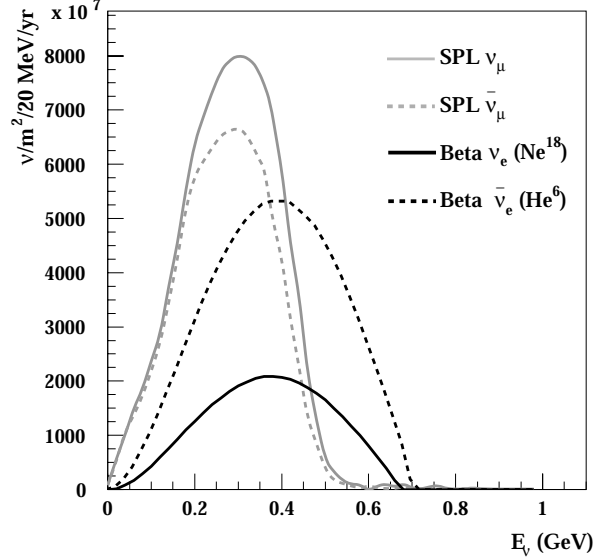


**Figure 6:** Neutrino flux of  $\beta$ -Beam ( $\gamma = 100$ ) and CERN-SPL SuperBeam, 3.5 GeV, at 130 Km of distance.

violation (at  $3\sigma$  level) if  $\delta_{\text{CP}} \geq 25^\circ$  and  $\theta_{13} \geq 1.4^\circ$  [124, 125]. The expected performances are shown in Fig. 8 and 13 along with those of other setups.

## 2.4 BetaBeams

BetaBeams have been introduced by P. Zucchelli in 2001 [97]. The idea is to generate pure, well collimated and intense  $\nu_e$  ( $\bar{\nu}_e$ ) beams by producing, collecting, accelerating radioactive ions and storing them in a decay ring in 10 ns long bunches, to suppress the atmospheric neutrino backgrounds. The resulting BetaBeam fluxes could be easily computed by the properties of the beta decay of the parent ion and by its Lorentz boost factor  $\gamma$  and would not be contaminated by unwanted neutrino flavours or helicities. The best ion candidates so far are  $^{18}\text{Ne}$  and  $^6\text{He}$  for  $\nu_e$  and  $\bar{\nu}_e$  respectively. The schematic layout of a Beta Beam is the following (see also Fig. 7):

**Ion production** Protons are delivered by a high power Linac. Beta Beam targets need 100  $\mu\text{A}$  proton beam, at energies between 1 and 2 GeV.

In case the Super Proton Linac (SPL) [116] would be used, Beta Beams could be fired to the same detector together with a neutrino SuperBeam [117]. SPL is designed to deliver 2mA of 2.2 GeV (kinetic energy) protons, in such a configuration Beta Beams would use 10% of the total proton intensity, leaving room to a very intense conventional neutrino beam.

The  $^6\text{He}$  target consists either of a water cooled tungsten core or of a liquid lead core which works as a proton to neutron converter surrounded by beryllium oxide [128], aiming for  $10^{15}$  fissions per second.  $^{18}\text{Ne}$  can be produced by spallation reactions, in this case protons will directly hit a magnesium oxide target. The collection and ionization of the ions is performed using the ECR technique [129].

This stage could be shared with nuclear physicists aiming to a source of radioactive ions of the same intensity to what needed by a Beta Beam. A design study has been recently approved by E.U.: Eurisol [127], where both nuclear and neutrino physics issues will be studied.

**Ion acceleration** The CERN PS and SPS can be used to accelerate the ions. There is a well established experience at CERN about ion accelerators. Ions are firstly accelerated to MeV/u by a Linac and to 300 MeV/u, in a single batch of 150 ns, by a rapid cycling synchrotron . 16 bunches



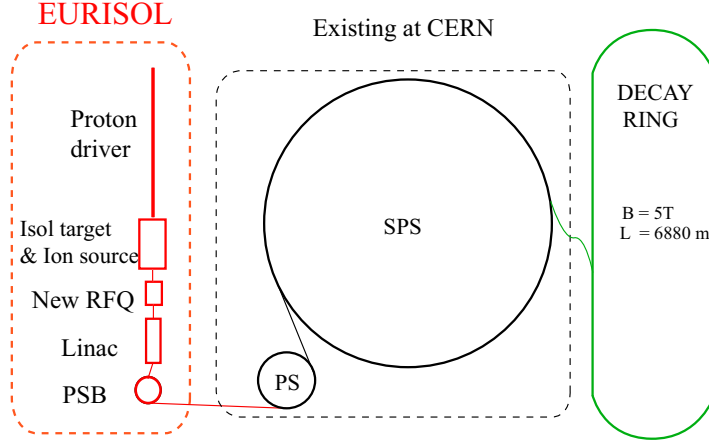


**Figure 7:** A schematic layout of the BetaBeam complex. At left, the low energy part is largely similar to the EURISOL project [127]. The central part (PS and SPS) uses existing facilities. At right, the decay ring has to be built.

(consisting of  $2.5 \cdot 10^{12}$  ions each in the case of  ${}^6\text{He}$ ) are then accumulated into the PS, and reduced to 8 bunches during their acceleration to intermediate energies. The SPS will finally accelerate the 8 bunches to the desired energy using a new 40 MHz RF system and the existing 200 MHz RF system, before ejecting them in batches of eight 10 ns bunches into the decay ring. The SPS could accelerate  ${}^6\text{He}$  ions at a maximum  $\gamma$  value of  $\gamma_{{}^6\text{He}} = 150$ .

**Decay ring** The decay ring has a total length of 6880 m and straight sections of 2500 m each (36% useful length for ion decays). These dimensions are fixed by the need to bend  ${}^6\text{He}$  ions up to  $\gamma = 150$  using 5 T superconducting magnets. Due to the relativistic time dilatation, the ion lifetimes reach several minutes, so that stacking the ions in the decay ring is mandatory to get enough decays and hence high neutrino fluxes. The challenge is then to inject ions in the decay ring and merge them with existing high density bunches. As conventional techniques with fast elements are excluded, a new scheme (asymmetric merging) was specifically conceived [130].

Summarizing, the main features of a neutrino beam based on the BetaBeams concept are:

- the beam energy depends on the  $\gamma$  factor. The ion accelerator can be tuned to optimize the sensitivity of the experiment;
- the neutrino beam contains a single flavor with an energy spectrum and intensity known a priori. Therefore, unlike conventional neutrino beams, close detectors are not necessary to normalize the fluxes;
- neutrino and anti-neutrino beams can be produced with a comparable flux;
- differently from SuperBeams, BetaBeams experiments search for  $\nu_e \rightarrow \nu_\mu$  transitions, requiring a detector capable to identify muons and separate them from electrons. Moreover, since the beam does not contain  $\nu_\mu$  or  $\bar{\nu}_\mu$  in the initial state, magnetized detectors are not needed. This is in contrast with the neutrino factories (see Sec.2.5) where the determination of the muon sign is mandatory.

A baseline study for a Beta Beam complex (Fig. 7) has been carried out at CERN [131]. The reference  $\beta\text{B}$  fluxes are  $5.8 \cdot 10^{18}$   ${}^6\text{He}$  useful decays/year and  $2.2 \cdot 10^{18}$   ${}^{18}\text{Ne}$  decays/year if a single ion specie circulates in the decay ring.

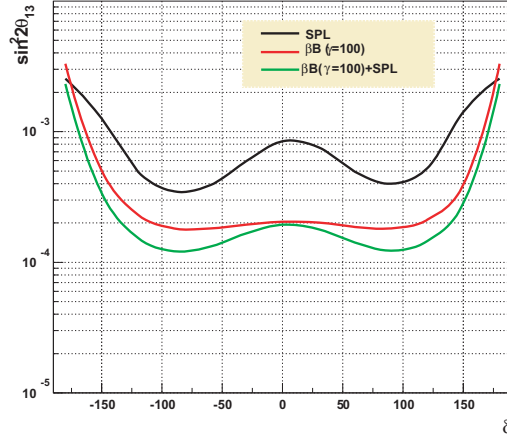


**Figure 8:**  $\theta_{13}$  sensitivity (90% CL) as function of  $\delta_{CP}$  for  $\Delta m_{23}^2 = 2.5 \cdot 10^{-3} eV^2$ ,  $\text{sign}(\Delta m_{23}^2) = 1$ , 2% systematic errors. SPL-SB sensitivities have been computed for a 10 years  $\nu_\mu$  run,  $\beta B$  and  $\beta B_{100,100}$  for a 10 years  $\nu_e + \bar{\nu}_e$  run. The SPL-SB 3.5 GeV, BetaBeam with  $\gamma = 100, 100$  and their combination are shown.

The water Čerenkov could be a suitable technology for a large detector. The physics potential has been initially computed in [132, 133] for  $\gamma_{He} = 60$ ,  $\gamma_{Ne} = 100$  and with a 440 kton detector at 130 km, Memphys, see also section 3.3.1.

The most updated sensitivities for the baseline Beta Beam are computed in a scheme where both ions are accelerated at  $\gamma = 100$ , the optimal setup for the CERN-Frejus baseline of 130 km, [134]. The  $\theta_{13}$  sensitivity curve, computed with a 6 parameters fit minimized over the solar and the atmospheric parameters and projected over  $\theta_{13}$ , is shown in Fig. 8 [134]. Degeneracies induced by the unknown values of  $\text{sign}(\Delta m_{23}^2)$  and  $\theta_{23}$  are not accounted for in these first plots.

The leptonic CP violation discovery potential (LCPV) has been computed with the following procedure. For any choice of a true value of  $\theta_{13}$ ,  $\bar{\theta}_{13}$ , a loop on test values of  $\delta_{CP}$ ,  $\bar{\delta}_{CP}$ , is initiated, until the fit around  $(\bar{\theta}_{13}, \bar{\delta}_{CP})$  is  $3\sigma$  away from any solution at  $\delta_{CP} = 0$  and  $\delta_{CP} = \pi$ . While in ref. [135] this procedure is performed in the full  $(\theta_{13}, \delta_{CP})$  space ( $3\sigma$  corresponding to  $\Delta\chi^2 = 11.8$ ), here the solution is searched having marginalized out  $\theta_{13}$  (GLoBES function `GblChiDelta` [136]). The LCPV at  $3\sigma$  ( $\Delta\chi^2 = 9.0$ ) is shown in Fig. 13. It takes into account all the parameter errors and all the possible degeneracies [134]. As it is common practice in literature  $\theta_{23} = 40^\circ$  has been used, to leave room for the octant ( $\pi/2 - \theta_{23}$ ) degeneracy. Each of the 4 true values of  $\text{sign}(\Delta m_{23}^2)$  and  $\theta_{23}$ : normal:  $\text{sign}(\Delta m_{23}^2) = 1$ ,  $\theta_{23} < \pi/4$ ; sign:  $\text{sign}(\Delta m_{23}^2) = -1$ ,  $\theta_{23} < \pi/4$ ; octant:  $\text{sign}(\Delta m_{23}^2) = 1$ ,  $\theta_{23} > \pi/4$ ; mixed:  $\text{sign}(\Delta m_{23}^2) = -1$ ,  $\theta_{23} > \pi/4$ . has been fitted with the 4 possible fit combinations, the worst case is then taken. Also shown are the leptonic CP violation discovery potentials neglecting the degenerate solutions (that is choosing the right combination of  $\text{sign}(\Delta m_{23}^2)$  and  $\theta_{23}$  for the fit). Effect of degeneracies are sometimes visible for high values of  $\theta_{13}$ , precisely the region where they can be reduced by a combined analysis with atmospheric neutrinos [137]. A quantitative computation of the combined analysis of Beta Beam and atmospheric neutrinos, as well as SPL superbeam and atmospheric neutrinos, has been recently shown in reference [138].

BetaBeams require a proton driver in the energy range of 1-2 GeV, 0.5 MWatt power. The SPL can be used as injector, at most 10% of its protons would be consumed. This allows a simultaneous  $\beta B$  and SPL-SB run, the two neutrino beams having similar neutrino energies (cfr. Fig. 6). The same detector could then be exposed to  $2 \times 2$  beams ( $\nu_\mu$  and  $\bar{\nu}_\mu \times \nu_e$  and  $\bar{\nu}_e$ ) having access to CP, T and

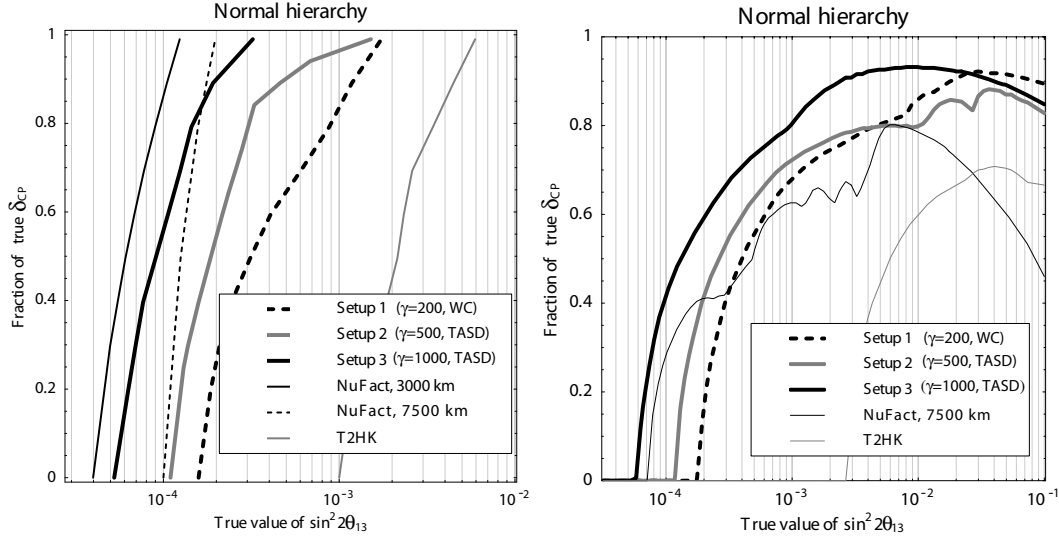


**Figure 9:** *LEFT: The  $\sin^2 2\theta_{13}$  discovery reach (including systematics and correlations) for different setups (the NO $\nu$ A TASD detector is described in Sections 2.2 and 3.1) as function of the true values of  $\sin^2 2\theta_{13}$  and  $\delta_{CP}$  ( $3\sigma$  confidence level). The values of  $\delta_{CP}$  are “stacked” to the fraction of  $\delta_{CP}$ , i.e.,  $\sin^2 2\theta_{13}$  will be discovered for a certain fraction of all possible values of  $\delta_{CP}$ . For a uniform probability contribution in  $\delta_{CP}$ , the fraction of  $\delta_{CP}$  directly corresponds to the probability to discover  $\sin^2 2\theta_{13}$ . RIGHT: The sensitivity to CP violation for the normal mass hierarchy for different experiments as function of the true values of  $\sin^2 2\theta_{13}$  and  $\delta_{CP}$  at the  $3\sigma$  confidence level. Both plots from reference [142]*

CPT violation searches in the same run. This is particularly important because CP and T channels would have different systematics and different backgrounds, allowing for independent checks of the same signal. Furthermore, the SPL  $\nu_\mu$  and  $\bar{\nu}_\mu$  beams would be the ideal tool to measure signal cross sections in the close detector.

With this combination of neutrino beams a sensitivity to  $\sin^2 2\theta_{13} \geq 2 \cdot 10^{-4}$  (90%CL) exploiting a CP violation discovery potential at  $3\sigma$  if  $\delta_{CP} \geq 18^\circ$  and  $\theta_{13} \geq 0.55^\circ$  [124]

BetaBeam capabilities for the maximum values of  $\gamma$  available with the SPS,  $\gamma^6\text{He} = 150$  have been computed in [139].

BetaBeam capabilities for ions accelerated at higher energies than those allowed by SPS have been first computed in [140] and subsequently in [139, 141, 142]. These studies assume that the same ion fluxes of the baseline scenario can be maintained. However, this is not the case if the number of stored bunches is kept constant in the storage ring. On the other hand, by increasing  $\gamma$  (i.e. the neutrino energy) the atmospheric neutrinos background constraint on the total bunch length [97] becomes less essential because of the reduced atmospheric neutrino flux at higher energies. Studies are in progress at CERN in order to define realistic neutrino fluxes as a function of  $\gamma$  [143].

The outcome of these studies shows anyway that higher energy Beta Beams have a CP discovery potential competitive with a neutrino factory, as shown in the plots of Fig. 9 [142].

It is worth noting that if a high intensity Beta Beam with  $\gamma \sim 300 \div 500$  (requiring a higher energy accelerator than SPS, like the Super-SPS [144]) can be built, a 40 kton iron calorimeter located at the Gran Sasso Laboratory will have the possibility to discover a non vanishing  $\delta_{CP}$  if  $\delta_{CP} > 20^\circ$  for  $\theta_{13} \geq 2^\circ$  (99% C.L.) and measure the sign of  $\Delta m_{23}^2$  [145].

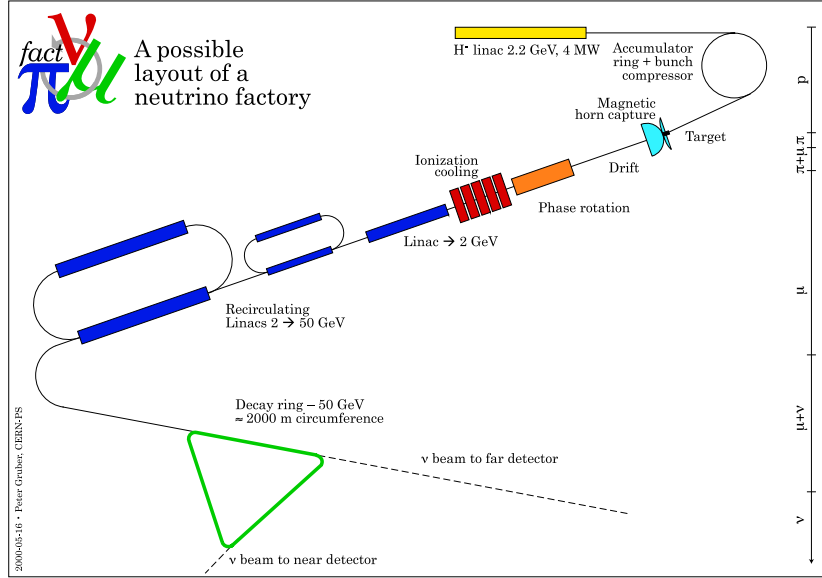


**Figure 10:** *Schematic layout of a Neutrino Factory.*

For a review on BetaBeams see also [146].

A very recent development of the Beta Beam concept is the conceptual possibility to have monochromatic, single flavor neutrino beams thanks to the electron capture process [147, 148]. A suitable ion candidate exists:  $^{150}\text{Dy}$ , whose performances have been already delineated [147].

## 2.5 The Neutrino Factory

<sup>3</sup> In a Neutrino Factory [150] muons are accelerated from an intense source to energies of several GeV, and injected in a storage ring with long straight sections. The muon decays:

$$\mu^+ \rightarrow e^+ \nu_e \bar{\nu}_\mu \quad \text{and} \quad \mu^- \rightarrow e^- \bar{\nu}_e \nu_\mu$$

provide a very well known flux with energies up to the muon energy itself. The overall layout is shown in Fig. 10.

Neutrino Factory designs have been proposed in Europe [151, 152], the US [153–155], and Japan [156]. Of these designs, the American one is the most developed, and we will use it as an example in general with a few exceptions. The conclusions of these studies is that, provided sufficient resources, an accelerator complex capable of providing about  $10^{21}$  muon decays per year can be built. The Neutrino Factory consists of the following subsystems:

**Proton Driver.** Provides 1-4 MW of protons on a pion production target. For the Neutrino Factory application the energy of the beam within 4-30 GeV is not critical, since it has been shown that the production of pions is roughly proportional to beam power. The time structure of the proton beam has to be matched with the time spread induced by pion decay (1-2 ns); for a Linac driver such as the SPL, this requires an additional accumulator and compressor ring.

**Target, Capture and Decay.** A high-power target sits within a 20T superconducting solenoid, which captures the pions. The high magnetic field smoothly decreases to 1.75T downstream of the target, matching into a long solenoid decay channel. A design with horn collection has been proposed at CERN for the Neutrino Factory, with the benefit that it can be also used for a SuperBeam design.

<sup>3</sup>Material for this Section is mainly taken from ref. [149]

**Table 5:** Comparison of unloaded Neutrino Factory costs estimates in M\$ for the US Study II design and improvement estimated for the latest updated US design (20 GeV/c muons). Costs are shown including A: the whole complex; B no Proton Driver and C: no proton driver and no Target station in the estimates. Table from Ref. [157].

Costs in M\$	A	B	C
Old estimate from Study II	1832	1641	1538
Multiplicative factor for new estimate	0.67	0.63	0.60

**Bunching and Phase Rotation.** The muons from the decaying pions are bunched using a system of RF cavities with frequencies that vary along the channel. A second series of RF cavities with higher gradients is used to rotate the beam in longitudinal phase-space, reducing the energy spread of the muons.

**Cooling.** A solenoid focusing channel with high-gradient 201 MHz RF cavities and either liquid-hydrogen or LiH absorbers is used to reduce the transverse phase-space occupied by the beam. The muons lose, by dE/dx losses, both longitudinal- and transverse-momentum as they pass through the absorbers. The longitudinal momentum is restored by re-acceleration in the RF cavities.

**Acceleration.** The central momentum of the muons exiting the cooling channel is 220 MeV/c. A superconducting Linac with solenoid focusing is used to raise the energy to 1.5 GeV. Thereafter, a Recirculating Linear Accelerator raises the energy to 5 GeV, and a pair of Fixed-Field Alternating Gradient rings accelerate the beam to at least 20 GeV.

**Storage Ring.** A compact racetrack geometry ring is used, in which 35% of the muons decay in the neutrino beam-forming straight section. If both signs are accelerated, one can inject in two superimposed rings or in two parallel straight sections. This scheme produces over  $6 \cdot 10^{20}$  useful muon decays per operational year and per straight section in a triangular geometry.

The European Neutrino Factory design is similar to the US design, but differs in the technologies chosen to implement the subsystems.

The Japanese design is quite different, and uses very large acceptance accelerators. Cooling, although it would improve performance, is not considered mandatory in this scheme.

An important Neutrino Factory R&D effort is ongoing in Europe, Japan, and the U.S. since a few years. Significant progress has been made towards optimizing the design, developing and testing the required components, and reducing the cost.

To illustrate this progress, the cost estimate for a recent update of the US design [157] is compared in Table 5 with the corresponding cost for the previous "Study II" US design [155]. In this design the Neutrino Factory would accelerate protons up to 20 GeV/c, with a flux of  $1.2 \cdot 10^{20}$  muon decays per straight section per year for a proton driver power of 1 MW ( $4.8 \cdot 10^{20}$   $\mu$  decays year at 4 MW).

It should be noted that the Study II design cost was based on a significant amount of engineering input to ensure design feasibility and establish a good cost basis. Neutrino Factory R&D has reached a critical stage in which support is required for two key international experiments (MICE [158] and Targetry [159]) and a third-generation international design study. If this support is forthcoming, a Neutrino Factory could be added to the Neutrino Physics roadmap by the end of the decade.

### 2.5.1 Oscillations physics at the Neutrino Factory

Considering a Neutrino Factory with simultaneous beams of positive and negative muons, 12 oscillation processes can in principle be studied, Table 6.

**Table 6:** *Oscillation processes in a Neutrino Factory*

$\mu^+ \rightarrow e^+ \nu_e \bar{\nu}_\mu$	$\mu^- \rightarrow e^- \bar{\nu}_e$	
$\bar{\nu}_\mu \rightarrow \bar{\nu}_\mu$	$\nu_\mu \rightarrow \nu_\mu$	disappearance
$\bar{\nu}_\mu \rightarrow \bar{\nu}_e$	$\nu_\mu \rightarrow \nu_e$	appearance (challenging)
$\bar{\nu}_\mu \rightarrow \bar{\nu}_\tau$	$\nu_\mu \rightarrow \nu_\tau$	appearance (atm. oscillation)
$\nu_e \rightarrow \nu_e$	$\bar{\nu}_e \rightarrow \bar{\nu}_e$	disappearance
$\nu_e \rightarrow \nu_\mu$	$\bar{\nu}_e \rightarrow \bar{\nu}_\mu$	appearance: “golden” channel
$\nu_e \rightarrow \nu_\tau$	$\bar{\nu}_e \rightarrow \bar{\nu}_\tau$	appearance: “silver” channel

Of course the neutrinos coming from decays of muons of different charge must not be confused with each other, this can be done by timing provided the storage ring is adequately designed.

One of the most striking features of the Neutrino Factory is the precision with which the characteristics of all components of the beam could be known. This was studied extensively in a CERN Report [160], where the following effects were considered

- beam polarization effects, and its measurement by a polarimeter, allowing extraction of the beam energy, energy spread and verification that the polarization effects on the neutrino fluxes average out to zero with high precision;
- beam divergence effects, with the preliminary, conceptual study of a Čerenkov device to monitor the angular distribution of muons in the beam [161]
- radiative effects in muon decay;
- absolute normalization to be obtained both from a beam monitor, with the added possibility of an absolute cross-section normalization using the inverse muon decay reaction,  $\nu_\mu e^- \rightarrow \mu^- \nu_e$ , in the near detector;

with the conclusion that, in principle, a normalization of fluxes and cross-sections with a precision of  $10^{-3}$  can be contemplated. Some of these features should also be present for a BetaBeam, and for any facility in which a stored beam of well defined optical properties is used to produce neutrinos. This is an essential difference with respect to the SuperBeams, where the knowledge of relative neutrino-vs-antineutrino cross-sections and fluxes will rely on the understanding of the initial particle production.

The Neutrino Factory lends itself naturally to the exploration of neutrino oscillations between  $\nu$  flavors with high sensitivity. The detector should be able to perform both appearance and disappearance experiments, providing lepton identification and charge discrimination which is a tag for the initial flavor and of the oscillation. In particular the search for  $\nu_e \rightarrow \nu_\mu$  transitions (“golden channel”) [162] appears to be very attractive at the Neutrino Factory, because this transition can be studied in appearance mode looking for  $\mu^-$  (appearance of wrong-sign  $\mu$ ) in neutrino beams where the neutrino type that is searched for is totally absent ( $\mu^+$  beam in  $\nu F$ ).

The emphasis has been placed so far on small mixing angles and small mass differences. With two 40 kton magnetic detectors (MINOS like) at 700 (or 7000) and 3000 km, with a conservative high

energy muon detection threshold of 5 GeV, exposed to both polarity beams and  $10^{21}$  muon decays, it will be possible to explore the  $\theta_{13}$  angle down to  $0.1^\circ$  opening the possibility to measure the  $\delta_{CP}$  phase [87, 162, 163], as it is shown by the plots of Fig.13.

On the other hand, the relative high energies of neutrinos selected by placing such a high threshold on muon energies require very long baselines (several thousands kilometers) for Neutrino Factories experiments, and at these baselines CP asymmetries are dominated by matter effects [164]. Taking advantage of the matter effects, such an experiment will determine unambiguously  $\text{sign}(\Delta m_{23}^2)$  for large enough  $\theta_{13}$  ( $\theta_{13} \geq 2^\circ$ ). However, we remind that, such as for other facilities, the determination of  $(\theta_{13}, \delta)$  at the Neutrino Factory is not free of ambiguities: up to eight different regions of the parameter space can fit the same experimental data. In order to solve these ambiguities, a single experimental point on a single neutrino beam is not enough.

One possibility at the Neutrino Factory is to make use of the rich flavour content of the beam. This imply an optimized network of detectors with different characteristics. Indeed, a specific disadvantage of the considered magnetized iron detector when dealing with degeneracies is the following: the lower part of the Neutrino Factory spectrum (say,  $E_\nu \in [0, 10]$  GeV) cannot be used due to the extremely low efficiency in this region of the detector. This part of the spectrum, on the other hand, is extremely useful to solve degeneracies, as it has been shown in several papers [165].

One possibility is to envisage that all of BetaBeams, SuperBeams and Neutrino Factories will be available. Several investigations on how to solve this problem have been carried out, as reported in [166] and references therein.

A more interesting but challenging task will be to assume that only one of these facilities will become available (a more economical assumption!) and to investigate its ability to solve these ambiguities.

There are several handles to this problem at a Neutrino Factory. Clearly one should use more than just the wrong sign muons. Such a study was performed assuming the feasibility of a liquid argon detector [170]. By separating the events into several classes, right sign muon, wrong sign muon, electron and neutral current; and by performing a fine energy binning down to low energies; it was shown that the matter resonance could be neatly measured as shown in Fig. 11. The simultaneous observation of the four aforementioned channels was shown to allow resolution of ambiguities to a large extent.

The tau appearance channel *silver channel* [167] has been advocated as a powerful means of solving ambiguities. This can be readily understood since this channel has the opposite-sign dependence on  $\delta_{CP}$  than the golden one, while having similar dependence on matter effects and  $\theta_{13}$ . Another channel to be used is the  $\nu_\mu$  disappearance channel, rather effective for large values of  $\theta_{13}$  [99]. The principle of degeneracies-solving using several baselines, binning in energies and both silver and golden channels is explained on Fig. 12. The full demonstration that a Neutrino Factory alone with a complete set of appropriate detectors and two baselines could unambiguously do the job remains however to be worked out.

According to Table 6, Neutrino Factory potential could be further improved with a detector capable of measuring the charge of the electrons. R&D efforts for a liquid argon detector embedded in a magnetic fields are ongoing [171]; the first curved tracks were recently observed in a 10 liters Liquid Argon TPC embedded in magnetic field [172].

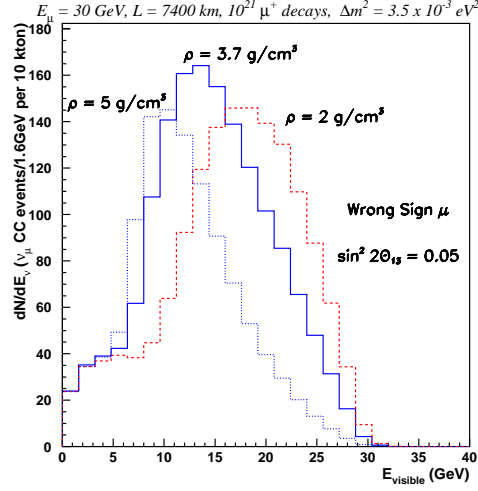


**Figure 11:** Variation of the MSW resonance peak for wrong sign muons as a function of Earth density. The plot is normalized to  $10^{21} \mu^+$  decays. From reference [170].

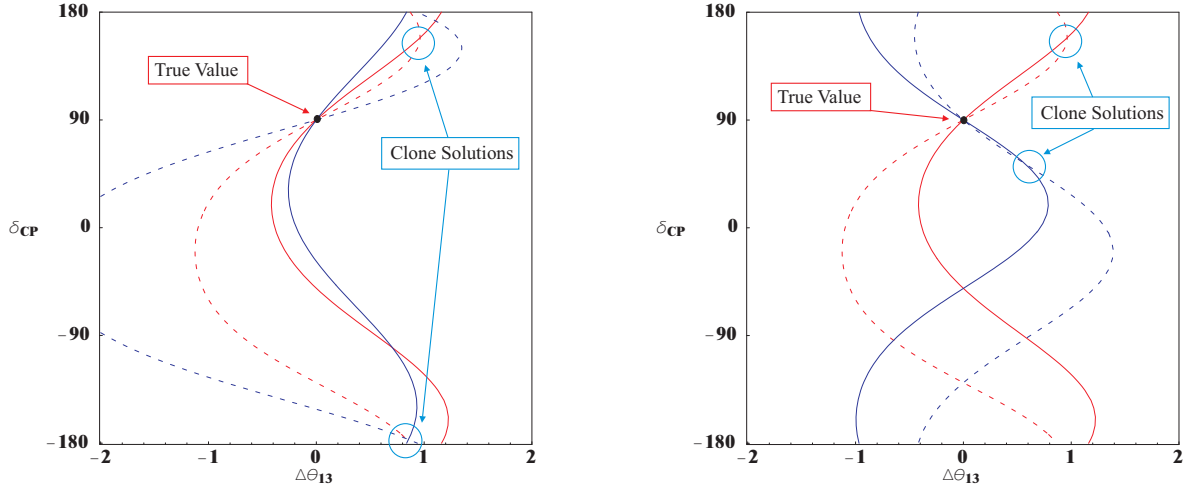


**Figure 12:** Solving the intrinsic degeneracy: two baseline  $L=730$  and  $3500$  km, same channel example on the left, vs two channels  $\nu_e \rightarrow \nu_\mu$  vs  $\nu_e \rightarrow \nu_\tau$  same baseline example on the right. From Ref. [168]

### 3 Research and development on detectors: status and priorities

#### 3.1 Low-Z Tracking Calorimetry

Low-Z Tracking Calorimetry optimizes the detection of electrons in the final state by using a fine sampling in terms of radiation lengths, leading to the choice for a low-Z passive material. This is the technique used for the study of  $\nu_\mu e^-$  scattering in the CHARM II experiment at CERN [101]. Here we discuss the status of the design of the NO $\nu$ A experiment proposed for the detection of  $\nu_\mu - \nu_e$  oscillations in the off-axis NuMI beam at Fermilab [100], with the observation of  $\theta_{13}$  as its prime aim.

The NO $\nu$ A detector foresees a mass one order of magnitude larger than MINOS [66] and at the same time, in relation to its aim, a finer sampling ( $\Delta X_0 < 0.3$  if particle board is used as passive



material, to be compared to 1.5 with MINOS, which has iron as the passive material). The principal technical issue is to improve the performance and substantially reduce the unitary cost of the trackers. The main technological innovation consists in the use of liquid scintillator read by Avalanche Photodiodes (APDs), instead of plastic scintillator read by multianode PMTs.

The detector finally chosen for NO $\nu$ A is a "Totally Active" Scintillator Detector (TASD), with a 30 kton mass, of which 24 kton are of liquid scintillator and the rest of PVC. In TASD, the scintillator modules have cells along the beam 6.0 cm long and 3.9 cm width. TASD consists of a single block with overall dimensions 15.7x15.7x132 m<sup>3</sup>. Lacking the particle board, the PVC must provide a self-supporting structure for a detector as high as a five-storey building. Since last year, progress has been made also in the mechanical design and in the assembling methods.

The electromagnetic energy resolution is  $\Delta E/E \sim 10\%/\sqrt{E(\text{GeV})}$ , the almost continuous pulse height information along the track helps in  $e/\pi^0$  discrimination.

The use of APDs results in a considerably lower cost than with PMTs. 2x16 pixel APDs are commercially produced in large quantities and already foreseen for the CMS experiment at LHC. The high quantum efficiency, about 85%, allows to have longer strips and less readout channels.

The No $\nu$ A design is in constant progress. If funding would begin in late 2006, the No $\nu$ A detector could be ready in 2011. It is worth noting that the progress with the development of the trackers is potentially useful also for magnetized iron spectrometers for neutrino factories or colliders.

### 3.2 Magnetized Iron Spectrometers

This technique is conventional, but the mass to be considered is one order of magnitude larger than for present magnetized iron spectrometers, like MINOS.

Recent studies indicates that a magnetized iron toroidal spectrometer of the required mass is feasible [111]. On one hand, the design of toroids with radius up to 10 m can be extrapolated from MINOS, with thicker plates for larger planes. On the other hand, the No $\nu$ A liquid scintillator technology with APD readout allows to have transverse dimensions twice as large than in MINOS. Such a detector concept permits direct use of the experience with MINOS.

The India Neutrino Observatory (INO) [112] foresees a dipole magnet equipped with RPCs, as in MONOLITH [113]. The INO basic motivation is the study of atmospheric neutrinos like with MONOLITH; a future use in a very long baseline experiment with a  $\nu$ -factory is envisaged. The investigations started with MONOLITH on the detector performance for design optimization have to be continued, in a comparison with other detectors.

A conceptual spectrometer based on a 40 kton iron solenoid magnetized at 1 T by a superconducting coil, with embedded solid scintillator rods as the active detectors, has been presented in Ref. [110]. Considerable more work is required to define its features and assess its practical feasibility.

In general, practical problems (mechanics, magnet design, etc.) must be thoroughly addressed. In addition, as already mentioned more simulation work is required in order to understand and optimize the performance by a proper choice of the main detector parameters.

### 3.3 Water Čerenkov

Water Čerenkovs can provide a very large target mass and, if the photo-sensors have a sufficient density, a sensitivity down to the low energies of solar neutrinos. Its capabilities concern  $\nu$  astrophysics,  $\nu$  oscillations and proton decay. Above a few GeV, DIS dominates over QE scattering and leads to frequent multi-ring events more complicated to reconstruct. A similar limitation in energy comes from difficulties in the  $e/\pi^0$  discrimination at high energies. The technique is not suitable at the high energies of  $\nu$ -factories, where, in addition, a muon charge measurement is needed. One should also

remark that the low neutrino cross-section at low energies reduces the advantage given by the very large mass which can be realized.

The detectors presently under study represent the third generation of successful detectors, with in each stage an increase by one order of magnitude in mass. The performance of Super-KamiokaNDE has been widely simulated and observed, providing a basis for a mass extrapolation by one order of magnitude. The performance as well as the limitations are well known, also from K2K and related tests.

Two detector designs are being carried out, namely Hyper-KamiokaNDE [102] and UNO [103]. The design of a detector to be located at Frejus (Memphys) has been also initiated.

Hyper-KamiokaNDE foresees two 500 kton modules placed sideways, each consisting of five 50 m long optical compartments. The cost is higher than for a single module, but maintenance with one module always alive and a staging in the detector construction become possible. The present design foresees about 200,000 20" PMTs, to be compared with 11,146 in Super-KamiokaNDE. The detector could be constructed in about 10 years, starting after a few years of T2K operation.

The UNO design provides a 650 kton mass subdivided into three optical compartments with different photo-sensor coverage. The central one has a 40% coverage as in Super-KamiokaNDE, allowing to pursue solar  $\nu$  studies. The side compartments have 10% coverage. The number of 20" PMTs is two times smaller than with 40% coverage for the full detector, but still amounts to 56,650. The question arises as to whether this subdivision, with its non-uniformity given by the lower coverage in  $\frac{2}{3}$  of the detector, is the optimal solution to reduce the global cost.

By giving appropriate aspect ratio and shape to the cavern, its realization does not seem a problem.

A large fraction of the total detector cost, reaching  $\sim \frac{1}{2}$  or more if PMTs are used, comes from the photo-sensors. The present cost of 100,000-200,000 20" PMTs is hard to cover. Moreover, their production would take about 8 years, leading also to storage problems. The main issue is thus the development and acquisition of photo-sensors at acceptable cost and production rate, as well as an improvement of their performance. A better time resolution would improve neutrino vertexing and single photon sensitivity would give better ring reconstruction. A strong collaboration with industry is essential, as for the development of 20" PMTs by Hamamatsu for KamiokaNDE and Super-KamiokaNDE.

The Hamamatsu 20" glass bulbs are manually blown by specially trained people. Automatic manufacturing does not seem a practical solution to reduce the cost and speed-up the production rate, as the required quantity is still small compared to commercial PMTs. The question is whether a size smaller than 20", with an appropriate coverage, is more practical and cost effective. With a smaller size, automatic bulb manufacturing is eased and the risk of implosion decreased, with a possible saving in the plastic protection to damp implosions. For R&D on PMTs, collaborations have been established with industries also in Europe (Photonis) and USA.

To explore alternatives to PMTs, studies on new photo-sensors have been launched. In addition to reduce cost, while improving production rate and performance, it is essential to achieve the long term stability and reliability which is proven for PMTs.

Hybrid Photo-Detectors (HPD) are being developed by Hamamatsu, in collaboration with ICRR of Tokyo University. The HPD glass envelope is internally coated with a photo-cathode and a light reflector. Electrons are accelerated by a very high voltage towards an Avalanche Diode (AD). The strong electron bombardment results in a high gain ( $\sim 4500$  for 20 kV voltage) in this first stage of amplification. It gives a remarkable single photon sensitivity and makes ineffective the AD thermally generated noise. The gain is lower than with PMTs, hence stable and highly reliable amplifiers are needed. The degradation in time resolution given by the transit time spread through the dynode chain is avoided, so that a  $\sim 1$  ns time resolution can be achieved, to be compared with the 2.3 ns of the 20"

PMTs. The cost reduction with respect to PMTs essentially comes from the use of solid state devices like the AD, avoiding the complicated PMT dynode structure.

The principle has been proved with a 5" HPD prototype. Successful results from tests of an 13" prototype operated with 12 kV are now available, showing a  $3 \cdot 10^4$  gain, good single photon sensitivity, 0.8 ns time resolution and a satisfactory gain and timing uniformity over the photo-cathode area. The next step will be the operation at a voltage up to 20 kV, giving a higher gain and a wider effective area of the photo-cathode. The development of HPD has been initiated also in Europe, in collaboration with Photonis.

### 3.3.1 The MEMPHYS detector

The MEMPHYS (MEgaton Mass Physics) detector is a Megaton-class water Čerenkov in the straight extrapolation of the well known and robust technique used for the Super-Kamiokande detector. It is designed to be located at Frejus, 130 km from CERN and it is an alternative design of the UNO [126] and Hyper-Kamiokande [94] detectors and shares the same physics case both from non accelerator domain (nucleon decay, SuperNovae neutrino from burst event or from relic explosion, solar and atmospheric neutrinos) and from accelerator (SuperBeam, BetaBeam) domain. For the physics part not covered by this document, this kind of megaton water detector can push the nucleon decay search up to  $10^{35}$  yrs in the  $e^+\pi^0$  channel and up to few  $10^{34}$  yrs in the  $K^+\bar{\nu}$  channel, just to cite these benchmark channels. MEMPHYS can register as many as 150,000 events from a SN at 10 kpc from our galaxy and 50 events or so from Andromeda. To detect relic neutrinos from past SuperNovae explosions one can use pure water and get a flux of 250 evts/10 y/500 kton or increase this number by a factor 10 by adding gadolinium salt.

A recent civil engineering pre-study to envisage the possibly of large cavity excavation located under the Frejus mountain (4800 m.e.w.) near the present Modane Underground Laboratory has been undertaken. The main result of this pre-study is that MEMPHYS may be built with present techniques as 3 or 4 shafts modular detector, 250000 m<sup>3</sup> each with 65 m in diameter, 65 m in height for the total water containment. Each of these shafts corresponds to about 5 times the present Super-Kamiokande cavity. For the present physical study, the fiducial volume of 440 kton which means 3 shafts and an Inner Detector (ID) of 57 m in diameter and 57 m in height is assumed. Each ID may be equipped with photodetectors (PMT, HPD,...) with a surface coverage at least 30%. The Frejus site, 4800 m.w.e, offers a natural protection against cosmic rays by a factor  $10^6$ .

The decision for cavity digging is fixed at 2010 after an intense Detector Design Study (eg. cavity excavation, photodetector R&D) performed in parallel of the digging of at least a Safety Gallery in the Frejus road tunnel. One may note that this key date may also be decisive for SPL construction as well as for the choice of the EURISOL site. After that, the excavation and PMT production are envisaged to take seven years or so, and the non accelerator program can start before the rise up of the accelerator program (SuperBeam and BetaBeam) which may start before 2020.

A first estimate of the costs of such a detector is reported in Table 7

### 3.4 Liquid Argon Time Projection Chamber

The Liquid Argon Time Projection Chamber (LAr TPC) provides an excellent imaging device and a dense neutrino target. It is a true "electronic bubble chamber" with a much larger mass (3 ton for Gargamelle, up to 100 kton now envisaged for LAr TPCs). The "state of the art" is given by the 300 ton T300 ICARUS [104] prototype module, tested at ground level in Pavia but not yet used in an experiment.

**Table 7:** Preliminary cost estimate of the MEMPHYS detector

3 Shafts	240 ME
Total cost of 250k 12" PMTs	250 ME
Infrastructure	100 ME
Total	590 ME

Two mass scales are foreseen for future experiments. For close  $\nu$  detectors in Super-Beams, a mass of the order of 100 ton is envisaged. Detectors with 50-100 kton masses are proposed for  $\nu$  oscillation,  $\nu$  astrophysics and proton decay [105] [106] [107], implying a step in mass by more than two orders of magnitude with respect to the T300 ICARUS module.

Cryogenic insulation imposes a minimal surface/volume ratio. The modular ICARUS approach has thus to be abandoned for a single very large cryogenic module with about 1:1 aspect ratio.

To limit the number of readout channels, drift lengths have to be longer than the 1.5 m of the T300 module. The LAr TPC envisaged for the off-axis NuMI beam [105] [106] foresees 3 m drift lengths with readout conceptually as in ICARUS. In another approach [107], the very strong attenuation over a much longer drift length (20 m) is compensated by the so-called "Double Phase" amplification and readout [108], tested on the ICARUS 50 liter chamber [109]. In both cases, the signal attenuation imposes a liquid Argon contamination by electronegative elements at the 0.1 ppb level.

In Ref. [107] a 100 kton detector consisting of a single module both for cryogenics and readout has been proposed. The 20 m drift in a field raised to 1 kV/cm results in a 10 ms drift time. With a 2 ms electron live-time in liquid Argon, the 6000 electrons/mm signal is attenuated by  $e^{-t/\tau} \approx 1/150$  and becomes too low for a readout as in ICARUS. In the Double Phase readout, electrons are extracted from the liquid by a grid and multiplied in the gas phase using gas chamber techniques. The  $\sigma \approx 3$  mm spread from the diffusion in the 20 m drift gives an intrinsic limit to the readout granularity.

The design of the single large cryostat [107] can benefit from the techniques developed for transportation and storage of large quantities of liquefied natural gas, kept at boiling temperature by letting it evaporate. A large cryogenic plant is needed for the initial filling and for the continuous refilling to compensate the evaporation.

The R&D for the detector of Ref. [107] foresees: drift under 3 atm pressure as at the tank bottom; charge extraction and amplification; imaging devices; cryogenics and cryostat design, in collaboration with industry; a column-like prototype with 5 m drift and double-phase readout, with a 20 m drift simulated by a reduced E field and by a lower liquid Argon purity; test of a prototype in a magnetic field (as for use in a  $\nu$ -Factory); underground safety issues.

Tests on a 10 liter LAr TPC inserted in a 0.55 T magnetic field have been performed [114], together with a tentative layout for the implementation of a large superconducting solenoidal coil into the design of Ref. [107].

The experience accumulated in two decades with ICARUS is very important. However, a substantial R&D is required, at an extent which depends on the detector design and on the (underground) location. In the design of very large detectors, with or without magnetic field, one has to proceed from concepts or conceptual designs to a practical design.

### 3.5 The Emulsion Cloud Chamber

The use of Emulsion Cloud Chamber (ECC) has been proposed to detect "silver events" from  $\nu_e - \nu_\tau$  oscillations at a  $\nu$ -Factory, in order to complement the  $\nu_e - \nu_\mu$  "golden events" in resolving  $\theta_{13} - \delta$

ambiguities [115].

The ECC of the OPERA experiment [69] in the CNGS beam consists of a multiple sandwich of lead and nuclear emulsion sheets. The production and decay of  $\tau$  leptons is expected to be observed with a very low background thanks to the emulsion sub- $\mu\text{m}$  resolution. The 1.8 kton OPERA target is built up with about 200,000 lead-emulsion "bricks".

At the  $\nu$ -Factory, a 4 kton mass is envisaged. By scanning only "wrong sign" muons as those coming from  $\tau$  decays, the scanning load is expected to be comparable with that in OPERA. An increase in the speed of the automatic microscopes is foreseeable. The OPERA Collaboration is working to provide a milestone in the application of the ECC technique.

#### 4 Preliminary comparison of accelerator facilities

The comparison of performances of different facilities cannot be considered as concluded. Several different aspects still need to be clarified before a final comparison can be performed.

- Costs, timescales, fluxes of the different accelerators systems are not yet fully worked out.
- Performances and optimization of the detectors are not known at the same level: for water Čerenkov detectors full simulation and full reconstructions of the events are available, based on the experience of Super-Kamiokande, but the optimization in terms of photo-detector coverage is still to be performed. The optimization of the magnetic detector (and of the assumed cuts) for the Neutrino Factory was performed for very small values of  $\theta_{13}$ , and the performances are for the moment based on parametrization of the MINOS performances, and very low values of backgrounds from hadron decays (pions, kaons, and charm) are claimed possible. The performances of the emulsion detector for the silver channel of Nufact or of the liquid argon detector are based on full simulations, but will need to be bench-marked using the performances of OPERA and ICARUS respectively.
- Several different measurements can be defined as significant for the facility, and they cannot be optimized all together (see also reference [142]). For instance the following measurements bring to different optimizations: sensitivity to  $\theta_{13}$ , discovery of subleading  $\nu_\mu \rightarrow \nu_e$  oscillations, unambiguous measurement of  $\theta_{13}$ , measure of  $\text{sign}(\Delta m_{23}^2)$ , discovery of leptonic CP violation, unambiguous measurement of  $\delta_{\text{CP}}$ .
- The final extraction of the oscillation parameters can significantly change depending on technical aspects of the fitting programs (like choice of the input parameters, treatment of the errors on the neutrino oscillation parameters, treatment of degeneracies etc.).

The GLoBES program [136] represents a major improvement: it allows to compare different facilities keeping the same the fitting program, and it makes explicit the description of the performances of the detectors. We strongly recommend that new developments in this field will make use of GLoBES, in view of a more transparent comparison of the different proposals.

- Systematic errors that strongly influence performances, for instance sensitivity to leptonic CP violation for large values of  $\theta_{13}$ , are not substantially discussed in the literature. We are confident that facilities where neutrino fluxes can be known a-priori, as the case of Beta Beams and Neutrino Factories, will have smaller systematic errors (and smaller backgrounds) than e.g. neutrino SuperBeams. This difference is not known quantitatively today.

The concept of the near detector station(s) and flux monitoring systems has to be proposed together with the facility, in particular for low energy (few 100 MeV) BetaBeam and SuperBeam where the issues of muon mass effect, Fermi motion and binding energy uncertainty are highly non-trivial.

Finally, for the Neutrino Factory, the question of systematics on the prediction of matter effects is essential for the performance at large values of  $\theta_{13}$ .

- Overall performances will depend on the combination of several different inputs. For instance low energy Super Beams and Beta Beams can profit of atmospheric neutrino oscillations, detected with a large statistics in the gigantic water Čerenkov detector, to solve degeneracies and measure  $\text{sign}(\Delta m_{23}^2)$ , as shown in the [137]. Neutrino Factory can profit of the combination of different channels as the golden and the silver one (see Section 2.5), detectors at different baselines, atmospheric neutrinos collected in the the iron magnetized detector [173]. A full exploration of these possibilities is an ongoing process and the results available at today cannot be considered final.

Having said that, a comparison of the facilities that at present are described in the GLoBES library [174], as far as concerns and leptonic CP violation discovery potential, is shown in Fig. 13.

The plots show the sensitivity to CP violation at  $3\sigma$  CL ( $\Delta\chi^2 = 9$ ). Sensitivity to CP violation is defined, for a given point in the  $\theta_{13}$ - $\delta_{\text{CP}}$  plane, by being able to exclude  $\delta_{\text{CP}} = 0$  and  $\delta_{\text{CP}} = \pi$  at the given confidence level. All plots have been prepared with GLoBES [136].

Degeneracies and correlations are fully taken into account. For all setups the appropriate disappearance channels have been included. The Beta Beam is lacking muon neutrino disappearance, but the result does not change if T2K disappearance information is included in the analysis. In all cases systematics between neutrinos, anti-neutrinos, appearance and disappearance is uncorrelated. For all setups with a water Čerenkov detector the systematics applies both to background and signal, uncorrelated.

The Neutrino Factory assumes  $3.1 \cdot 10^{20} \mu^+$  decays per year for 10 years and  $3.1 \cdot 10^{20} \mu^-$  decays for 10 years. It has one detector with  $m=100$  kton at 3000 km and another 30 kton detector at 7000 km. The density errors between the two baselines are uncorrelated, sensitivities are computed for 2% and 5% systematic error on matter density. The systematics are 0.1% on the signal and 20% on the background, uncorrelated. The detector threshold and the other parameters are taken from [165] and approximate the results of [169].

The Beta Beam assumes  $5.8 \cdot 10^{18} {}^6\text{He}$  decays per year for five years and  $2.2 \cdot 10^{18} {}^{18}\text{Ne}$  decays per year for five years. The detector mass is 500 kton. The detector description and the globes-file is from [134].

The SPL setup is taken from [125], and the detector mass is 500 kton.

The T2HK setup is taken from [165] and closely follows the LoI [94]. The detector mass is 1000 kton and it runs with 4MW beam power, 6 years with anti-neutrinos and 2 years with neutrinos. The systematic error on both background and signal is 5%.

The oscillation parameters were [175, 176]:  $\delta m_{23}^2 = 0.0024 \text{ eV}^2$ ,  $\delta m_{12}^2 = 0.00079 \text{ eV}^2$ ,  $\theta_{23} = \pi/4$ ,  $\theta_{12} = 0.578$ . The input errors are (at  $1\sigma$ ): 10% on  $\delta m_{23}^2$ , 10% on  $\theta_{23}$ , 10% on  $\theta_{12}$ , 4% on  $\delta m_{12}^2$ , 5% on  $\rho$  (unless otherwise stated).

## References

- [1] K. Hirata *et al.* (Kamiokande-II), Phys. Rev. Lett. **58**, 1490 (1987).

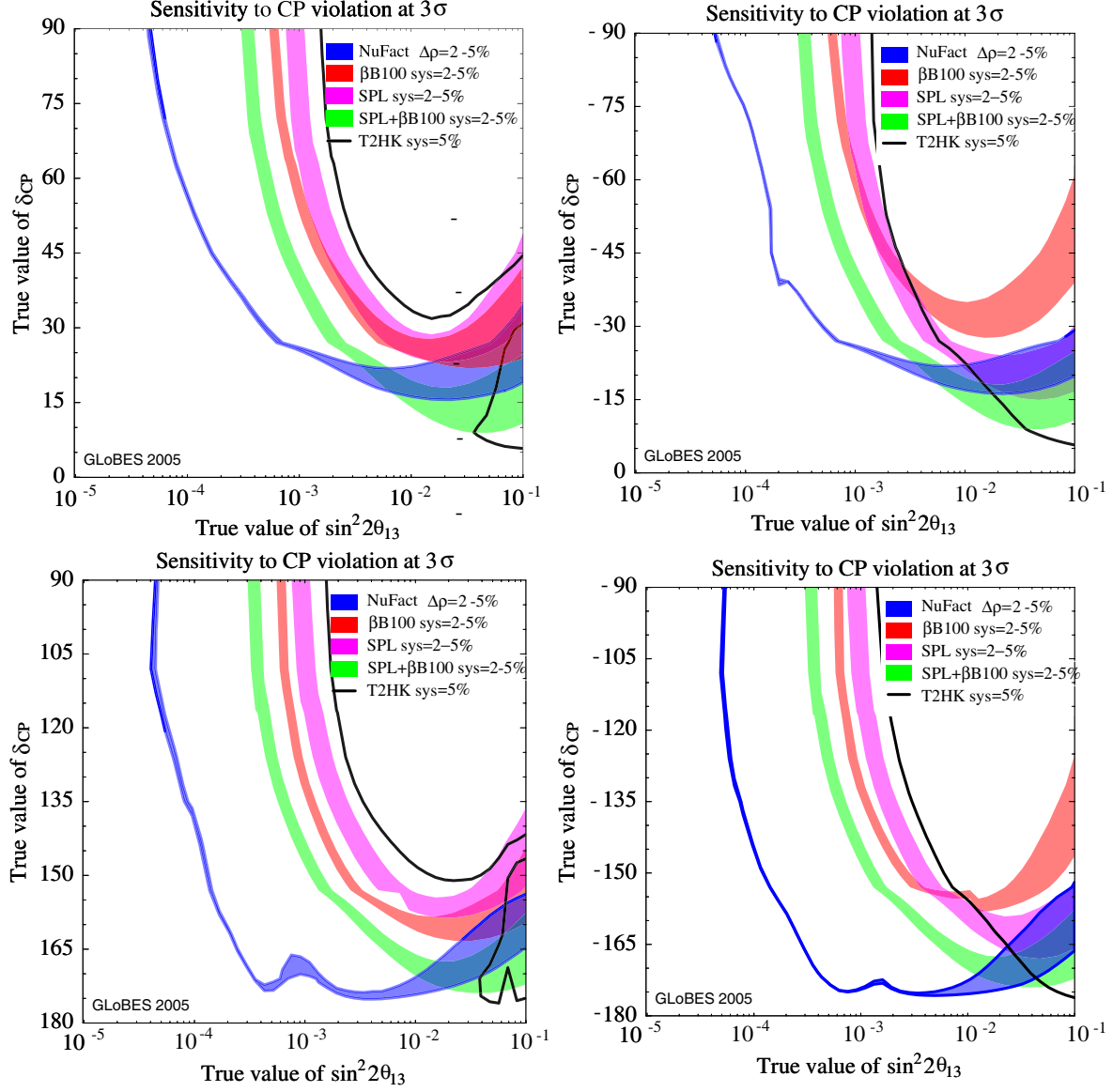


**Figure 13:**  $\delta_{CP}$  discovery potential at  $3\sigma$  (see text) computed for 10 years running time. For explanation of the facilities see the text. The four plots represent the four possible quadrants of  $\delta_{CP}$  values, performances of the different facilities are not at all the same in the different quadrants. The width of the curves reflects the range of systematic errors: 2% and 5% on signal and background errors for SPL-SB and Beta Beam, 2% and 5% for the matter density. Other systematic errors are 5% on signal and background of T2HK, 0.1% for nufact signal, 20% for nufact backgrounds. Description of the facilities can be found in [174]

- [2] R. M. Bionta *et al.*, Phys. Rev. Lett. **58**, 1494 (1987).
- [3] G. G. Raffelt, Ann. Rev. Nucl. Part. Sci. **49**, 163 (1999), hep-ph/9903472.
- [4] Y. Fukuda *et al.* (Super-K), Phys. Rev. Lett. **81**, 1562 (1998), hep-ex/9807003.
- [5] Q. R. Ahmad *et al.* (SNO), Phys. Rev. Lett. **89**, 011301 (2002), nucl-ex/0204008.
- [6] K. Eguchi *et al.* (Kamland), Phys. Rev. Lett. **90**, 021802 (2003), hep-ex/0212021.
- [7] M. H. Ahn *et al.* (K2K), Phys. Rev. Lett. **90**, 041801 (2003), hep-ex/0212007.
- [8] E. Aliu *et al.* (K2K), Phys. Rev. Lett. **94**, 081802 (2005), hep-ex/0411038.
- [9] M. C. Gonzalez-Garcia and Y. Nir, Rev. Mod. Phys. **75**, 345 (2003), hep-ph/0202058.
- [10] A. Aguilar *et al.* (LSND), Phys. Rev. **D64**, 112007 (2001), hep-ex/0104049.
- [11] B. Armbruster *et al.* (KARMEN), Phys. Rev. **D65**, 112001 (2002), hep-ex/0203021.
- [12] J. Wolf (KARMEN) Prepared for International Europhysics Conference on High- Energy Physics (HEP 2001), Budapest, Hungary, 12-18 Jul 2001.
- [13] K. Hagiwara *et al.*, Physical Review D **66**, 010001+ (2002), URL <http://pdg.lbl.gov>.
- [14] V. Barger, D. Marfatia, and K. Whisnant (2003), hep-ph/0308123.
- [15] G. L. Fogli, E. Lisi, A. Marrone, A. Palazzo, and A. M. Rotunno (2005), hep-ph/0506307.
- [16] R. N. Mohapatra (2002), hep-ph/0211252.
- [17] M.-C. Chen and K. T. Mahanthappa (2003), hep-ph/0305088.
- [18] R. N. Mohapatra (2003), hep-ph/0306016.
- [19] J. C. Pati (2003), hep-ph/0305221.
- [20] G. Altarelli and F. Feruglio (2003), hep-ph/0306265.
- [21] R. N. Mohapatra *et al.* (2005), hep-ph/0510213.
- [22] A. D. Dolgov, Phys. Rept. **370**, 333 (2002), hep-ph/0202122.
- [23] E. L. Wright (2003), astro-ph/0306132.
- [24] W. J. Percival *et al.* (The 2dFGRS Team) (2002), astro-ph/0206256.
- [25] S. Hannestad (2003), astro-ph/0303076.
- [26] P. Vogel (2000), nucl-th/0005020.
- [27] S. R. Elliott and P. Vogel, Ann. Rev. Nucl. Part. Sci. **52**, 115 (2002), hep-ph/0202264.
- [28] S. M. Bilenky, C. Giunti, J. A. Grifols, and E. Masso, Phys. Rept. **379**, 69 (2003), hep-ph/0211462.



- [29] M. Kobayashi and T. Maskawa, Prog. Theor. Phys. **49**, 652 (1973).
- [30] T. Ohlsson and H. Snellman, J. Math. Phys. **41**, 2768 (2000), hep-ph/9910546.
- [31] A. Cervera *et al.*, Nucl. Phys. **B579**, 17 (2000), hep-ph/0002108.
- [32] V. Barger, D. Marfatia, and K. Whisnant, Phys. Rev. **D65**, 073023 (2002), hep-ph/0112119.
- [33] C. Weinheimer, Nucl. Phys. Proc. Suppl. **118** (2003) 279.
- [34] V. M. Lobashev *et al.*, Nucl. Phys. Proc. Suppl. **91** (2001) 280. V. M. Lobashev, proceeding of “Neutrino Telescopes 2005”, Venice, pg. 507-517
- [35] KATRIN Coll., hep-ex/0109033.
- [36] A. Monfardini *et al.*, arXiv:hep-ex/0509038.
- [37] H. V. Klapdor-Kleingrothaus, A. Dietz and I. V. Krivosheina, Found. Phys. **32** (2002) 1181 [Erratum-ibid. **33** (2003) 679] [arXiv:hep-ph/0302248].
- [38] Y. G. Zdesenko, F. A. Danevich and V. I. Tretyak, Phys. Lett. B **546** (2002) 206.
- [39] A. M. Bakalyarov, A. Y. Balysh, S. T. Belyaev, V. I. Lebedev and S. V. Zhukov [C03-06-23.1 Collaboration], Phys. Part. Nucl. Lett. **2** (2005) 77 [Pisma Fiz. Elem. Chast. Atom. Yadra **2** (2005) 21] [arXiv:hep-ex/0309016].
- [40] C. Arnaboldi *et al.*, Phys. Rev. Lett. **95** (2005) 142501 [arXiv:hep-ex/0501034].
- [41] R. Arnold *et al.* [NEMO Collaboration], arXiv:hep-ex/0507083.
- [42] R. Ardito *et al.*, arXiv:hep-ex/0501010.
- [43] S. Schonert *et al.* [GERDA Collaboration], Nucl. Phys. Proc. Suppl. **145** (2005) 242.
- [44] For a recent review see: M. Fukugita, arXiv:hep-ph/0511068.
- [45] Precision Electroweak Measurements on the Z Resonance The LEP collaborations, hep-ex/0509008, to appear as physics report.
- [46] B. T. Cleveland *et al.*, Astrophys. J. **496** (1998) 505.
- [47] M. Altmann *et al.* [GNO Collaboration], Phys. Lett. B **490** (2000) 16 [arXiv:hep-ex/0006034].
- [48] J. N. Abdurashitov *et al.* [SAGE Collaboration], J. Exp. Theor. Phys. **95** (2002) 181 [Zh. Eksp. Teor. Fiz. **122** (2002) 211] [arXiv:astro-ph/0204245].
- [49] S. Fukuda *et al.* [Super-Kamiokande Collaboration], Phys. Lett. B **539** (2002) 179 [arXiv:hep-ex/0205075].
- [50] S. R. Ahmad *et al.*, [SNO Collaboration], nucl-ex/0204008. S. N. Ahmed *et al.* [SNO Collaboration], Phys. Rev. Lett. **92** (2004) 181301 [arXiv:nucl-ex/0309004].
- [51] K. Eguchi *et al.* [KamLAND Collaboration], Phys. Rev. Lett. **90** (2003) 021802 [arXiv:hep-ex/0212021]. T. Araki *et al.* [KamLAND Collaboration], Phys. Rev. Lett. **94** (2005) 081801 [arXiv:hep-ex/0406035].

- [52] Y. Fukuda *et al.* [Super-Kamiokande Collaboration], Phys. Rev. Lett. **81** (1998) 1562 [arXiv:hep-ex/9807003].
- [53] M. C. Sanchez *et al.* [Soudan 2 Collaboration], Phys. Rev. D **68** (2003) 113004 [arXiv:hep-ex/0307069].
- [54] M. Ambrosio *et al.* [MACRO Collaboration], Phys. Lett. B **566** (2003) 35 [arXiv:hep-ex/0304037].
- [55] Y. Ashie *et al.* [Super-Kamiokande Collaboration], Phys. Rev. Lett. **93** (2004) 101801 [arXiv:hep-ex/0404034].
- [56] M. Apollonio *et al.* [CHOOZ Collaboration], Eur. Phys. J. C **27** (2003) 331, [arXiv:hep-ex/0301017].
- [57] E. Aliu *et al.* [K2K Collaboration], Phys. Rev. Lett. **94** (2005) 081802 [arXiv:hep-ex/0411038].
- [58] L. Wolfenstein, Phys. Rev. D **17** (1978) 2369. S.P. Mikheev and A.Y. Smirnov, Nuovo Cim. C **9** (1986) 17.
- [59] see for instance P. Lipari, Phys. Rev. D **64** (2001) 033002 [arXiv:hep-ph/0102046].
- [60] G. L. Fogli, E. Lisi, A. Marrone and A. Palazzo, arXiv:hep-ph/0506083.
- [61] A. Aguilar *et al.* [LSND Collaboration], Phys. Rev. D **64** (2001) 112007 [arXiv:hep-ex/0104049].
- [62] B. Armbruster *et al.* [KARMEN Collaboration], Phys. Rev. D **65** (2002) 112001 [arXiv:hep-ex/0203021].
- [63] P. Astier *et al.* [NOMAD Collaboration], Phys. Lett. B **570** (2003) 19 [arXiv:hep-ex/0306037].
- [64] E. Church *et al.* [BooNe Collaboration], arXiv:nucl-ex/9706011.
- [65] A. Guglielmi, M. Mezzetto, P. Migliozzi and F. Terranova, arXiv:hep-ph/0508034.
- [66] E. Ables *et al.* [MINOS Collaboration], Fermilab-proposal-0875 G. S. Tzanakos [MINOS Collaboration], AIP Conf. Proc. **721**, 179 (2004).
- [67] The Fermilab NuMI Group, “NumI Facility Technical Design Report”, Fermilab Report NuMI-346, 1998.
- [68] F. Arneodo *et al.* [ICARUS Collaboration], Nucl. Instrum. and Meth. A **461** (2001) 324; P. Aprili *et al.*, “The ICARUS experiment”, CERN-SPSC/2002-27, SPSC-P-323.
- [69] OPERA Collaboration, CERN-SPSC-P-318, LNGS-P25-00; H. Pessard [OPERA Collaboration], arXiv:hep-ex/0504033. M. Guler *et al.* [OPERA Collaboration], “OPERA: An appearance experiment to search for  $\nu_\mu \rightarrow \nu_\tau$  oscillations in the CNGS beam. Experimental proposal,” CERN-SPSC-2000-028.
- [70] G. Acquistapace *et al.*, “The CERN neutrino beam to Gran Sasso”, CERN 98-02, INFN/AE-98/05 (1998); CERN-SL/99-034(DI), INFN/AE-99/05 Addendum.

- [71] H. W. Atherton *et al.*, “Precise measurements of particle production by 400 GeV/c protons on Beryllium targets,” CERN-80-07.
- [72] G. Ambrosini *et al.* [NA56/SPY Collaboration], *Eur. Phys. J. C* **10** (1999) 605.
- [73] L. Casagrande *et al.*, “The alignment of the CERN West Area neutrino facility,” CERN-96-06.
- [74] A. Guglielmi and G. Collazuol, “Monte Carlo Simulation of the SPS WANF Neutrino Flux”, INFN/AE-03/05 (2003).  
P. Astier *et al.* [NOMAD Collaboration], *Nucl. Instrum. Meth. A* **515** (2003) 800 [arXiv:hep-ex/0306022].
- [75] A. Ferrari, A. Guglielmi and P. R. Sala, *Nucl. Phys. Proc. Suppl.* **145** (2005) 93 [arXiv:hep-ph/0501283].
- [76] Report to the Fermilab Director by the Proton Committee, November 9, 2004, [http://www.fnal.gov/directorate/programplanning/Nov2004PACPublic/Draft\\_Proton\\_Plan\\_v2.pdf](http://www.fnal.gov/directorate/programplanning/Nov2004PACPublic/Draft_Proton_Plan_v2.pdf)
- [77] M. Komatsu, P. Migliozi and F. Terranova, *J. Phys. G* **29** (2003) 443 [arXiv:hep-ph/0210043].
- [78] P. Migliozi and F. Terranova, *Phys. Lett. B* **563** (2003) 73 [arXiv:hep-ph/0302274].
- [79] M. Benedikt, K. Cornelis, R. Garoby, E. Metral, F. Ruggiero and M. Vretenar, “Report of the High Intensity Protons Working Group,” CERN-AB-2004-022-OP-RF.
- [80] F. Ardellier *et al.* [Double-CHOOZ Collaboration], arXiv:hep-ex/0405032.
- [81] P. Huber, J. Kopp, M. Lindner, M. Rolinec and W. Winter, arXiv:hep-ph/0601266.
- [82] A. De Rujula, M.B. Gavela, P. Hernandez, *Nucl. Phys. B* **547** (1999) 21, arXiv: hep-ph/9811390.
- [83] ‘ECFA/CERN studies of a European Neutrino Factory complex’, A. Blondel et al, ed CERN 2004-002 (2004) <http://preprints.cern.ch/cernrep/2004/2004-002/2004-002.html>
- [84] Beams for European Neutrino Experiments is a Networking Activity (<http://bene.na.infn.it/>) supported by the EC and most major European Agencies in the framework of the FP6 Integrated Activity CARE (Coordinated Accelerator R&D in Europe) <http://esgard.lal.in2p3.fr/Project/Activities/Current/>. The scope of BENE is also described in more detail in the following document: <http://esgard.lal.in2p3.fr/Project/Activities/Current/Networking/N3/BENE-downsized-11.doc>
- [85] Workshop on Physics at a Multi Megawatt Proton driver, CERN-SPSC-2004-SPSC-M-722,
- [86] B. Richter, SLAC-PUB-8587 [arXiv:hep-ph/0008222], and references therein.
- [87] J. Burguet-Castell, M. B. Gavela, J. J. Gomez-Cadenas, P. Hernandez and O. Mena, *Nucl. Phys. B* **608** (2001) 301 [arXiv:hep-ph/0103258].
- [88] K. Kimura, A. Takamura and H. Yokomakura, *Phys. Rev. D* **66** (2002) 073005 [arXiv:hep-ph/0205295]. E. K. Akhmedov, R. Johansson, M. Lindner, T. Ohlsson and T. Schwetz, *JHEP* **0404** (2004) 078 [arXiv:hep-ph/0402175]. M. Freund, *Phys. Rev. D* **64** (2001) 053003 [arXiv:hep-ph/0103300].

- [89] H. Minakata and H. Nunokawa, JHEP **0110** (2001) 001 [arXiv:hep-ph/0108085].
- [90] V. Barger, D. Marfatia and K. Whisnant, Phys. Rev. D **65** (2002) 073023 [arXiv:hep-ph/0112119].
- [91] G. L. Fogli and E. Lisi, Phys. Rev. D **54** (1996) 3667 [arXiv:hep-ph/9604415].
- [92] M.G. Catanesi *et al.* [HARP Collaboration], CERN-SPSC/2001-017, SPSC/P322, May 2001.
- [93] M. G. Catanesi *et al.* [HARP Collaboration], arXiv:hep-ex/0510039.
- [94] Y. Itow *et al.*, “The JHF-Kamiokande neutrino project”, arXiv:hep-ex/0106019.
- [95] The E889 Collaboration, ”Long Baseline Neutrino Oscillation Experiment at the AGS”, Brookhaven National Laboratory Report BNL No. 52459, April 1995. A. Para and M. Szleper, arXiv:hep-ex/0110032.
- [96] S. Geer, Phys. Rev. D **57** (1998) 6989 [Erratum-ibid. D **59** (1999) 039903], [hep-ph/9712290].
- [97] P. Zucchelli, Phys. Lett. B **532** (2002) 166.
- [98] H. Minakata, M. Sonoyama and H. Sugiyama, Phys.Rev.D70:113012,2004; hep-ph/0406073. A. Donini, D. Meloni and S. Rigolin, hep-ph/0506100.
- [99] A. Donini, E. Fernandez-Martinez, D. Meloni and S. Rigolin, arXiv:hep-ph/0512038.
- [100] D. S. Ayres *et al.* [NOvA Collaboration], arXiv:hep-ex/0503053.
- [101] D. Geiregat et al., Nucl. Instr. and Meth., A 325 (1993) 92
- [102] K. Nakamura, Int. Journal of Mod. Phys. A 18 (2003) 4053, and references therein
- [103] UNO Proto Coll., SBHEP-01-03 (2000) Waseda Univ. (1992)
- [104] ICARUS Coll., LNGS-P28/2001 and ICARUS-TM/2001-03, hep-ex/0103008
- [105] FLARE Collaboration, Letter of Intent hep-ex/0408121 (2004)
- [106] D. Cline et al., Nucl. Instr. and Meth. A503 (2003) 136
- [107] A. Rubbia, Proc. of the II Int. Workshop on Neutrinos in Venice, Venice (2003)
- [108] B. A. Dolgoshein et al., Fiz. El. Chast. Atom. Yad. 4 (1973) 167
- [109] D. Cline et al., Astroparticle Physics 12 (2000) 373
- [110] A. Cervera et al., Nucl. Instr. and Meth. A451 (2000) 123
- [111] J. Nelson, proceedings of Nufact 05, LNF (Italy), 21-26 June 2005.
- [112] N.K. Mondal, proceedings of Nufact 05, LNF (Italy), 21-26 June 2005.
- [113] P. Antonioli, for the MONOLITH Coll., Nucl. Phys. (Proc. Suppl.) 100 (2001) 142
- [114] A. Rubbia, proceedings of Nufact 05, LNF (Italy), 21-26 June 2005.

- [115] A. Donini, D. Meloni and P. Migliozi, hep-ph/0206034
- [116] B. Autin *et al.*, CERN-2000-012
- [117] J. J. Gomez-Cadenas *et al.*, Proceedings of “Venice 2001, Neutrino telescopes”, vol. 2\*, 463-481, arXiv:hep-ph/0105297. A. Blondel *et al.*, Nucl. Instrum. Meth. A **503** (2001) 173. M. Mezzetto, J. Phys. G **29** (2003) 1771 [arXiv:hep-ex/0302005].
- [118] M. Apollonio *et al.*, arXiv:hep-ph/0210192.
- [119] L. Mosca, Nucl. Phys. Proc. Suppl. **138** (2005) 203.
- [120] J. E. Campagne and A. Cazes, arXiv:hep-ex/0411062.
- [121] R. Garoby, “The SPL at CERN,” CERN-AB-2005-007.
- [122] S. Gilardoni et al, AIP Conf. Proc. **721** (2004) 334.
- [123] A. Blondel et al, CERN-NUFACT-Note-78 (2001)
- [124] M. Mezzetto, Nucl. Phys. Proc. Suppl. **149** (2005) 179.
- [125] J.E. Campagne, hep-ex/0511005.
- [126] C. K. Jung [UNO Collaboration] arXiv:hep-ex/0005046.
- [127] <http://www.ganil.fr/eurisol/>
- [128] J. Nolen, NPA 701 (2002) 312c
- [129] P. Sortais, presentations at the Moriond workshop on radioactive beams, Les Arcs (France) 2003 “ECR technology”, <http://moriond.in2p3.fr/radio>
- [130] M. Benedikt, S. Hancock and J-L. Vallet, CERN note AB-Note-2003-080 MD
- [131] B. Autin *et al.*, arXiv:physics/0306106. M. Benedikt, S. Hancock and M. Lindroos, Proceedings of EPAC 2004, <http://accelconf.web.cern.ch/AccelConf/e04>.
- [132] M. Mezzetto, J.Phys. G **29** (2003) 1781 [arXiv:hep-ex/0302007]. J. Bouchez, M. Lindroos and M. Mezzetto, AIP conference proceedings, **721** (2003) 37 [arXiv:hep-ex/0310059].
- [133] A. Donini, E. Fernandez-Martinez, P. Migliozi, S. Rigolin and L. Scotto Lavina, Nucl. Phys. B **710** (2005) 402 [arXiv:hep-ph/0406132].
- [134] M. Mezzetto, Nucl. Phys. Proc. Suppl. **155** (2006) 214 [arXiv:hep-ex/0511005].
- [135] A. Donini, E. Fernandez-Martinez and S. Rigolin, Phys. Lett. B **621** (2005) 276 [arXiv:hep-ph/0411402].
- [136] P. Huber, M. Lindner and W. Winter, Comput. Phys. Commun. **167** (2005) 195 [arXiv:hep-ph/0407333].o
- [137] P. Huber, M. Maltoni and T. Schwetz, Phys. Rev. D **71** (2005) 053006 [arXiv:hep-ph/0501037]. R. Gandhi, P. Ghoshal, S. Goswami, P. Mehta and S. Uma Sankar, arXiv:hep-ph/0506145.

- [138] J. E. Campagne, M. Maltoni, M. Mezzetto and T. Schwetz, arXiv:hep-ph/0603172.
- [139] J. Burguet-Castell, D. Casper, E. Couce, J. J. Gomez-Cadenas and P. Hernandez, arXiv:hep-ph/0503021.
- [140] J. Burguet-Castell *et al.*, Nucl. Phys. B **695** (2004) 217 [arXiv:hep-ph/0312068].
- [141] F. Terranova, A. Marotta, P. Migliozi and M. Spinetti, Eur. Phys. J. C **38** (2004) 69 [arXiv:hep-ph/0405081].
- [142] P. Huber *et al.*, arXiv:hep-ph/0506237.
- [143] M. Lindroos, EURISOL DS/TASK12/TN-05-02, M. Lindroos, proceedings of Nufact 05.
- [144] O. Bruning *et al.*, “LHC luminosity and energy upgrade: A feasibility study,” CERN-LHC-PROJECT-REPORT-626.
- [145] A. Donini, E. Fernandez-Martinez, P. Migliozi, S. Rigolin, L. Scotto Lavina, T. Tabarelli de Fatis and F. Terranova, arXiv:hep-ph/0604229.
- [146] M. Mezzetto, Nucl. Phys. Proc. Suppl. **143** (2005) 309 [arXiv:hep-ex/0410083]. C. Volpe, arXiv:hep-ph/0605033.
- [147] J. Bernabeu, J. Burguet-Castell, C. Espinoza and M. Lindroos, hep-ph/0505054
- [148] J. Sato, hep-ph/0503144.
- [149] A. Blondel, proceedings of Nufact 05, in press.
- [150] S. Geer, Phys. Rev. D **57** (1998) 6989; A. De Rujula, M.B. Gavela and P. Hernandez, Nucl. Phys. B **547** (1999) 21; A. Blondel *et al.*, Nucl. Instrum. Methods Phys. Res., A **451** (2000) 102; J. J. Gomez-Cadenas and D.A. Harris, “Physics opportunities at neutrino factories,” Ann. Rev. Nucl. Part. Sci. **52** (2002) 253 and the annual proceedings of the International Nufact Workshop.
- [151] B. Autin, A. Blondel and J. Ellis eds, CERN yellow report CERN 99-02, ECFA 99-197
- [152] P. Gruber *et al.*, ‘The Study of a European Neutrino Factory Complex’, Neutrino Factory Note 103(2002) CERN/PS/2002-080(PP) , in ‘ECFA/CERN Studies of a European Neutrino Factory Complex ’ Blondel, A (ed.) *et al.* CERN-2004 002.- ECFA-04-230, p7
- [153] The Muon Collider and Neutrino Factory Collaboration, see the web site <http://www.cap.bnl.gov/mumu/> which contains also references to several physics studies.
- [154] Feasibility Study on a Neutrino Source Based on a Muon Storage Ring, D.Finley, N.Holtkamp, eds. (2000), <http://www.fnal.gov/projects/muon Collider/reports.html>
- [155] “Feasibility Study-II of a Muon-Based Neutrino Source”, S. Ozaki, R. Palmer, M. Zisman, and J. Gallardo, eds. BNL-52623, June 2001, available at <http://www.cap.bnl.gov/mumu/studyii/FS2-report.html> ; M.M. Alsharo’a *et al.*, Phys. Rev. ST Accel. Bemas **6**, 081001 (2003).
- [156] A Feasibility Study of A Neutrino Factory in Japan, Y. Kuno, ed., <http://www-prism.kek.jp/nufactj/index.html>

- [157] "Neutrino Factory and Beta Beam Experiments and Developments", (Eds. S. Geer and M. Zisman), Report of the Neutrino Factory and Beta Beam Working Group, APS Multi-Divisional Study of the Physics of Neutrinos, July 2004.
- [158] The International Muon Ionization Experiment MICE, <http://hep04.phys.iit.edu/cooldemo>
- [159] R.J. Bennett et al, 'Studies of a target system for a 4MW 24 GeV proton beam', CERN-INTC proposal 2003-033, April 2004.
- [160] A. Blondel et al eds., *ECFA/CERN studies of a European Neutrino Factory complex*, CERN 2004-002 (2004) <http://preprints.cern.ch/cernrep/2004/2004-002/2004-002.html>
- [161] A. Broncano and O. Mena, Eur.Phys.J. C29 (2003) 197-206; hep-ph/0203052
- [162] A. Cervera et al, Nucl.Phys.B579:17-55,2000, Erratum-ibid.B593:731-732,2001; hep-ph/0002108
- [163] P. Huber and W. Winter; Phys. Rev. D68, 037301(2003); hep-ph-0301257.
- [164] S. Geer, Comments Nucl. Part. Phys. A 2 (2002) 284 [arXiv:hep-ph/0008155].
- [165] P. Huber, M. Lindner and W. Winter, Nucl.Phys.B645:3-48,2002; hep-ph/0204352
- [166] A. Donini, AIP Conf. Proc. **721** (2004) 219 [arXiv:hep-ph/0310014].
- [167] A. Donini, D. Meloni, P. Migliozzi, Nucl. Phys. B646 (2002) 321, hep-ph/0206034; D. Autiero et al., Eur. Phys. J. C **33** (2004) 243 [arXiv:hep-ph/0305185].
- [168] S. Rigolin, Rencontres de Moriond 2004, hep-ph/0407009.
- [169] A. Cervera, F. Dydak and J. Gomez Cadenas, Nucl. Instrum. Meth. A **451** (2000) 123.
- [170] A. Bueno, M. Campanelli, A. Rubbia, Nucl. Phys. B **589** (2000) 577 [arXiv:hep-ph/0005007].
- [171] A. Ereditato and A. Rubbia, arXiv:hep-ph/0510131.
- [172] A. Badertscher et al, physics/0505151.
- [173] R. Gandhi, P. Ghoshal, S. Goswami, P. Mehta and S. Uma Sankar, arXiv:hep-ph/0411252. S. Choubey and P. Roy, Phys. Rev. D **73** (2006) 013006 [arXiv:hep-ph/0509197].
- [174] <http://www.hep.ph.ic.ac.uk/%7Elongkr/UKNF/Scoping-study/ISS-www-site/WG1-PhysPhen/Workshops/2005-11/AEDL/AEDL-Catalogue.htm>
- [175] M. Maltoni, T. Schwetz, M.A. Tortola, J.W.F. Valle, New J.Phys.6:122,2004, [hep-ph/0405172].
- [176] G.L. Fogli, E. Lisi, A. Marrone, A. Palazzo, A.M. Rotunno, hep-ph/0506307.